PALEOCEANOGRAPHY, VOL. 15, NO. 4, PAGES 425-442, AUGUST 2000

Potential links between surging ice sheets, circulation changes, and the Dansgaard-Oeschger cycles in the Irminger Sea, 60-18 kyr

S. van Kreveld,[1] M. Sarnthein,[1] H. Erlenkeuser,[2] P. Grootes,[2] S. Jung, [1,3]
M.J. Nadeau, [2] U. Pflaumann,[1] and A. Voelker[1,2]

Abstract. Surface and deepwater paleoclimate records in Irminger Sea core SO82-5 (59°N, 31°W) and Icelandic Sea core PS2644 (68°N, 22°W) exhibit large fluctuations in thermohaline circulation (THC) from 60 to 18 calendar kyr B.P., with a dominant periodicity of 1460 years from 46 to 22 calendar kyr B.P., matching the Dansgaard-Oeschger (D-O) cycles in the Greenland Ice Sheet Project 2 (GISP2) temperature record [*Grootes and Stuiver*, 1997]. During interstadials, summer sea surface temperatures (SST_{su}) in the Irminger Sea averaged to 8°C, and sea surface salinities (SSS) averaged to ~36.5, recording a strong Irminger Current and Atlantic THC. During stadials, SST_{su} dropped to 2°-4°C, in phase with SSS drops by ~1-2. They reveal major meltwater injections along with the East Greenland Current, which turned off the North Atlantic deepwater convection and hence the heat advection to the north, in harmony with various ocean circulation and ice models. On the basis of the IRD composition, icebergs came from Iceland, east Greenland, and perhaps Svalbard and other northern ice sheets. However, the southward drifting icebergs were initially jammed in the Denmark Strait, reaching the Irminger Sea only with a lag of 155-195 years. We also conclude that the abrupt stadial terminations, the D-O warming events, were tied to iceberg melt via abundant seasonal sea ice and brine water formation in the meltwater-covered northwestern North Atlantic. In the 1/1460-year frequency band, benthic $\delta^{18}O$ brine water spikes led the temperature maxima above Greenland and in the Irminger Sea by as little as 95 years. Thus abundant brine formation, which was induced by seasonal freezing of large parts of the northwestern Atlantic, may have finally entrained a current of warm surface water from the subtropics and thereby triggered the sudden reactivation of the THC. In summary, the internal dynamics of the east Greenland ice sheet may have formed the ultimate pacemaker of D-O cycles.

1. Introduction

Ice core studies show that the air temperatures over Greenland oscillated rapidly and frequently between cold and warm during isotope stages 3 and 2 [*Dansgaard et al.*, 1982, 1993; *Greenland Ice Core Project Members*, 1993; *Grootes et al.*, 1993; *Grootes and Stuiver*, 1997]. These Dansgaard-Oeschger (D-O) cycles somehow follow a dominant periodicity of ~1500 years [*Grootes and Stuiver*, 1997]. Each cycle is asymmetric, characterized by a rapid warming lasting a few decades or less [*Alley et al.*, 1993; *Dansgaard et al.*, 1993], a moderate cooling over ~500-1000 years subsequent to the peak interstadial, and a final abrupt cooling that leads to the next cold episode lasting ~500 years. The air temperature variations over the Greenland ice sheet have been found to closely match the changes in both North Atlantic sea surface temperature [*Bond et al.*, 1993; *Fronval et al.*, 1995] and deepwater circulation [*Rasmussen et al.*, 1997]. Progressively colder D-O cycles in North Atlantic surface temperature are bundled into some major so-called Bond cycles, with asymmetrical sawtooth shape, each ending with a major cold phase, the "Heinrich" events [*Bond et al.*, 1993].

The D-O cycles were attributed to various forcing mechanisms which may be external (e.g., solar/lunar variability) [*Keeling*, 1998] or internal (e.g., sea level changes), which may comprise the thermohaline circulation (THC) with or without ice sheet dynamics [*Broecker et al.*, 1990, 1992; *MacAyeal*, 1993a, b; *Alley and MacAyeal*, 1994; *Broecker*, 1994], or internal ocean-atmosphere interactions to the climate system [*Cane*, 1998].

On the basis of Heinrich layers of ice-rafted debris (IRD) [*Heinrich*, 1988; *Broecker et al.*, 1992; *Bond et al.*, 1992; *Grousset et al.*, 1993], *Broecker et al.* [1990] first claimed that the rapid climate variability was forced by Heinrich glacier surges from Labrador, stopping the North Atlantic THC, which draws warm, salty waters and heat from the tropics to high latitudes via the Gulf Stream and its extension, the North Atlantic Drift, a model further developed by *MacAyeal* [1993a, b]. These Heinrich IRD layers are most pronounced in a belt between Newfoundland and Europe at 40°-55°N and 10°-60°W [*Grousset et al.*, 1993], which is also matching a distinct $\delta^{18}O$ meltwater tongue [*Cortijo et al.*, 1997]. After each Heinrich event (HE), the THC resumed, leading into an abrupt warming, as shown by a subsequent D-O event. The HE occurred at 5-10 kyr intervals [*Bond et al.*, 1992, 1993];

[1]Institut für Geowissenschaften, Christian-Albrechts Universität, Kiel, Germany.
[2]Leibniz-Labor für Altersbestimmung und Isotopenforschung, Christian-Albrechts Universität, Kiel, Germany.
[3]Research School of Sedimentary Geology, Center for Marine Earth Sciences, Free University, Amsterdam, The Netherlands.

Paper number 1999PA000464.
0883-8305/00/1999PA000464$12.00

with more precise datings they focus more clearly to a mean of 7.2±2.4 kyr [*Sarnthein et al.*, 2000]. A similar frequency of IRD events was recorded for the past 500 kyr B.P. [*McManus et al.*, 1999]. In contrast, the northern ice sheets discharged iceberg flotillas more frequently, up to every 1-3 kyr [*Bond and Lotti*, 1995; *Stein et al.*, 1996; *Lackschewitz and Wallrabe-Adams*, 1997; *Elliot et al.*, 1998; *Lackschewitz et al.*, 1998; *Voelker et al.*, 1998].

In this paper, we assess the actual frequency and tracks of iceberg production in high latitudes and the potential impact of their meltwater on the sea surface temperature and salinity in the Irminger Basin and on Atlantic THC. Moreover, we study the characteristics of the more gradual cooling and abrupt warming along with D-O cycles to test the robustness of their 1500-year periodicity. We also examine whether the IRD events precede or follow the gradual D-O coolings (in the sense of *Bond and Lotti* [1995]). In the second case, *Bond and Lotti* [1995] and *Bond et al.* [1997] suggested that the D-O coolings would reflect a recurrent climate-driven mechanism, yet unknown, independent of ice discharge. We, however, focus on the surge-induced meltwater pulses that actually have governed the Atlantic THC system.

Our results rely on foraminifera-based data of sea surface temperature (SST), sea surface salinity (SSS), ice-rafted lithic grains (IRD), planktic and epibenthic stable isotopes at centennial to decadal resolution from 60 to 18 kyr B.P. in sediment core SO82-5 from the Irminger Sea (59°N, 31°W; 1416 m water depth; Figure 1). We compare these marine data with the Greenland Ice Sheet Project 2 (GISP2) $\delta^{18}O$ record [*Grootes et al.*, 1993; *Grootes and Stuiver*, 1997] of air temperatures at the Greenland ice summit (Figure 2). The causal links between the various atmospheric and marine climate signals are inferred from the phase leads and lags within the 1/1460-year frequency band.

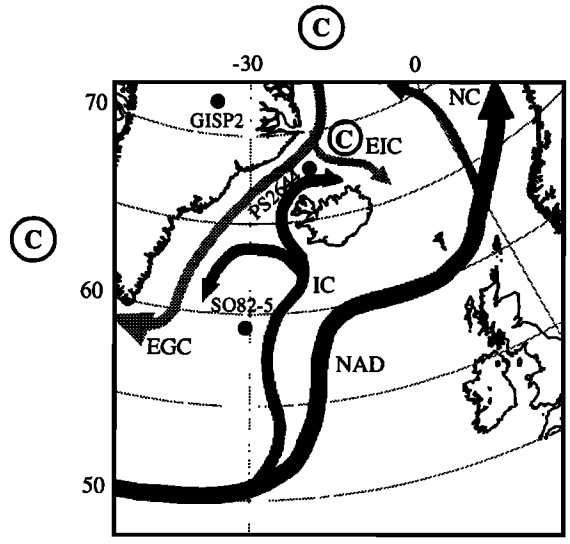

Figure 1. Location of sediment cores SO82-5 (59°N, 31°W; 1416 m water depth) and PS2644 (68°N, 22°W; 780 m water depth) and GISP2 ice core (73°N, 39°W; 3200 m above sea level) and modern surface circulation in the North Atlantic [*Dietrich et al.*, 1975; *Trangeled*, 1974]. EGC, East Greenland Current; EIC, East Icelandic Current, IC, Irminger Current; NAD, North Atlantic Drift; NC, Norwegian Current. C represents major convection cells.

Site SO82-5 was chosen because of its high sedimentation rates, averaging 11 cm/kyr [*Lackschewitz et al.*, 1998], its position near to the Irminger Current, and its proximity to the present-day polar front and the Greenland GISP2 ice core, where extreme natural climate variability was ideally documented between 60 and 18 kyr [*Grootes and Stuiver*, 1997].

Site SO82-5, which is situated to the south of the Denmark Strait, monitors the amount of icebergs derived from Icelandic and east Greenland sources. The site lies outside, north of the immediate trajectory of icebergs originating from Canada, the "Heinrich IRD belt" [*Grousset et al.*, 1993; *Cortijo et al.*, 1997].

In addition, our conclusions rely on gravity core PS2644 (68°N, 22°W; Figures 1 and 3), which was retrieved from the southern Icelandic Sea at 800 m depth. This site is monitoring variations in the incursion of warm water along with the northerly branch of the Irminger Current and the iceberg drift along with the East Greenland and East Iceland Currents. The paleoceanographic data sets obtained from this core are described in great detail by *Voelker* [1999].

2. Material and Methods

Gravity core SO82-5 was recovered from the western flank of the Reykjanes Ridge during the RV *Sonne* cruise SO82 in 1992 [*Endler and Lackschewitz*, 1993]. The morphology of the core site, the sedimentary structures, and the PARASOUND bundled echo sounder data suggest a sedimentary record free of turbidites. In the core sections covering $\delta^{18}O$ stage 3 and midstage 2 [*Lackschewitz et al.*, 1998], we sampled every 5 centimeter from 90 to 120 centimeter and every single cm between 120 and 540 cm, using 5 cm^3 plastic syringes, resulting in an average time resolution of 80 years. The bias of bioturbational mixing can be largely ignored at this subpolar site since the low carbon (and nutrient) flux characteristic for this environment reduces the bioturbational mixing depth to ~2 cm or less [*Trauth et al.*, 1997]. After freeze-drying, the samples were weighed to determine the dry bulk density, washed through a 63-μm sieve, and then dry-sieved at 150 μm. The fraction >150 μm was repeatedly split until enough specimens remained to identify and count between 300 and 1000 specimens of planktic foraminifera and 300 and 500 lithic grains. High-IRD concentrations (number per gram of dry sediment), which serve as a measure of iceberg advection, as suggested by *Broecker et al.* [1992] and *Bond et al.* [1992], generally match high concentrations of foraminifera.

The oxygen and carbon stable isotopes were measured on samples of at least 30 specimens of *Neogloboquadrina pachyderma* (sinistral) (150-250 μm). The tests were treated with 99.8% ethanol, cracked, and ultrasonically cleaned for 1 min. The samples were dissolved with H_3PO_4 in the automated Carbo-Kiel preparation line, and the released CO_2 gas was measured online using a Finnigan MAT-251 mass spectrometer at the Leibniz Laboratory of Kiel University. The analytical precision of the internal carbonate standard (Solnhofen Limestone), which was run every 10 samples, was 0.07‰ for $\delta^{18}O$ and 0.05‰ for $\delta^{13}C$. The isotope values were calibrated to the Peedee belemnite (PDB) scale using NBS 20.

The epibenthic *Cibicidoides wuellerstorfi* $\delta^{18}O$ and $\delta^{13}C$ data are mostly from *Jung* [1996], with additional data from

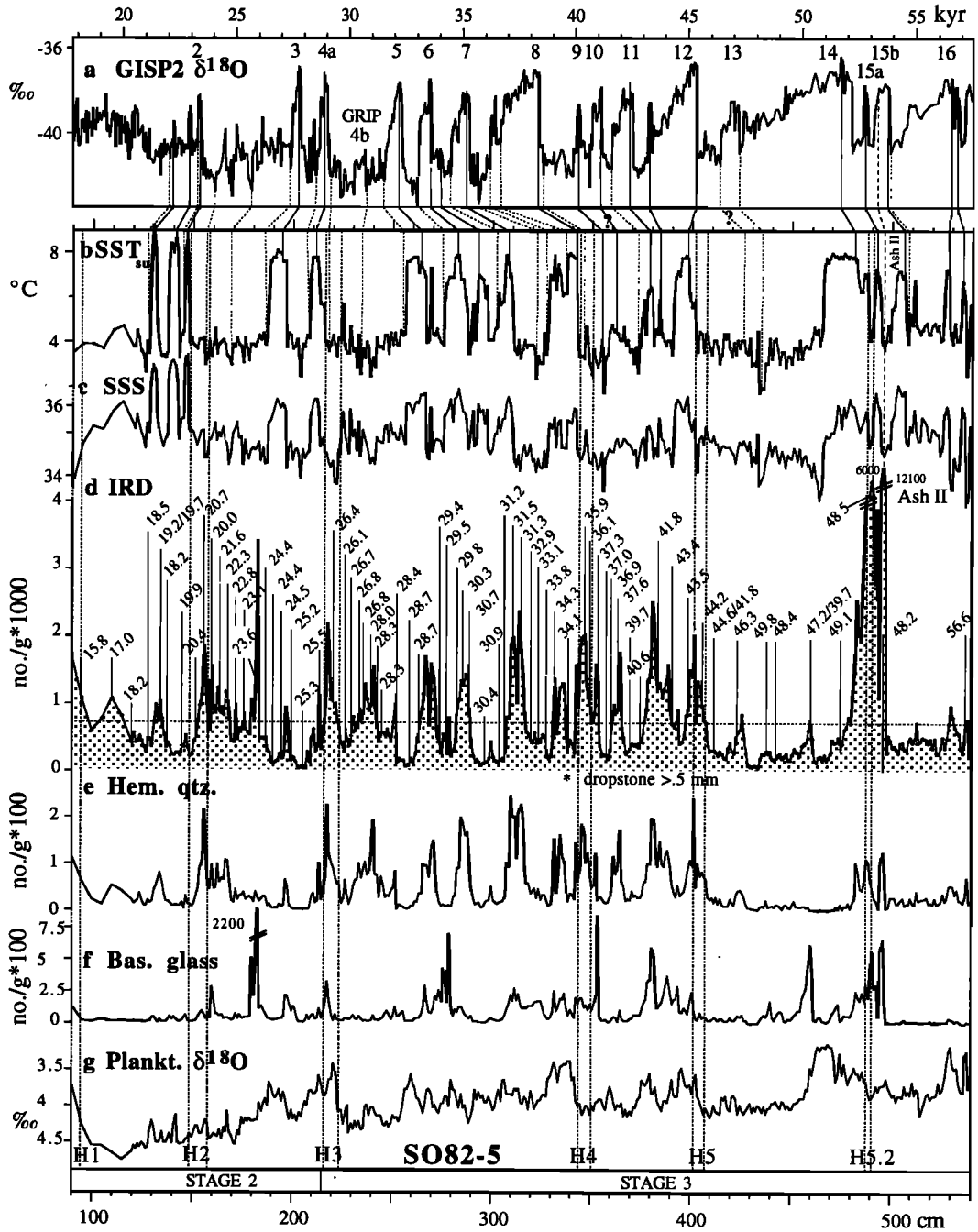

Figure 2. (a) 1m resolution GISP2 $\delta^{18}O$ data of temperature changes on Greenland Summit [*Grootes et al.*, 1993; *Grootes and Stuiver*, 1997] correlated to various climate records in core SO82-5 plotted against depth. (b) Summer sea surface temperatures (SST_{su}) derived from planktic foraminiferal counts. Lines indicate major tie points, and numbers 2-16 refer to Dansgaard-Oeschger interstadials [*Johnsen et al.*, 1992]. Correlations were drawn considering the new 20 cm resolution GISP2 $\delta^{18}O$ record (see Figure 5, [*Stuiver and Grootes*, 2000]). Number 4b indicates a short-term warming identified in core SO82-5 such as in the Summit ice cores [*Dansgaard et al., 1993*; *Grootes et al.*, 1993]. (c) Sea surface salinity (SSS) record estimated using a ratio of $\delta^{18}O_{water}$ to SSS of 1:1.79 [GEOSECS Atlantic, 1987]. (d) Concentration of ice-rafted debris (IRD) and its components, (e) hematite-covered quartz (Hem. qtz.), and (f) basaltic (Bas.) glass expressed as number of grains >150 μm per gram dry sediment. (g) The $\delta^{18}O$ record of planktic *N. pachyderma* (s.) (Plankt. $\delta^{18}O$). Horizontal dotted line in Figure 2d shows the mean concentration of 800 ice-rafted debris grains per gram dry sediment. Numbers show ^{14}C ages in kiloyears B.P. (-400 years) measured on *N. pachyderma* (s.) (Table 1). Stippled bars mark Heinrich events H1-H5.2, defined by the low-SST and high-IRD intervals preceding D-O events 1, 2, 4, 8, 12, and 14 (H5.2 was first identified in cores from Rockall Plateau [*Sarnthein et al.*, 2000]). Age correlation between GISP2 and the SST record is roughly constrained by 71 accelerator mass spectrometry (AMS) ^{14}C datings and finally based on numerous tie points, correlating the end of abrupt SST warmings with the onset of D-O interstadials (solid lines) and the beginning of SST lows with the onset of D-O stadials (dashed lines). Further tie points correlate the stadial extremes with SST minima.

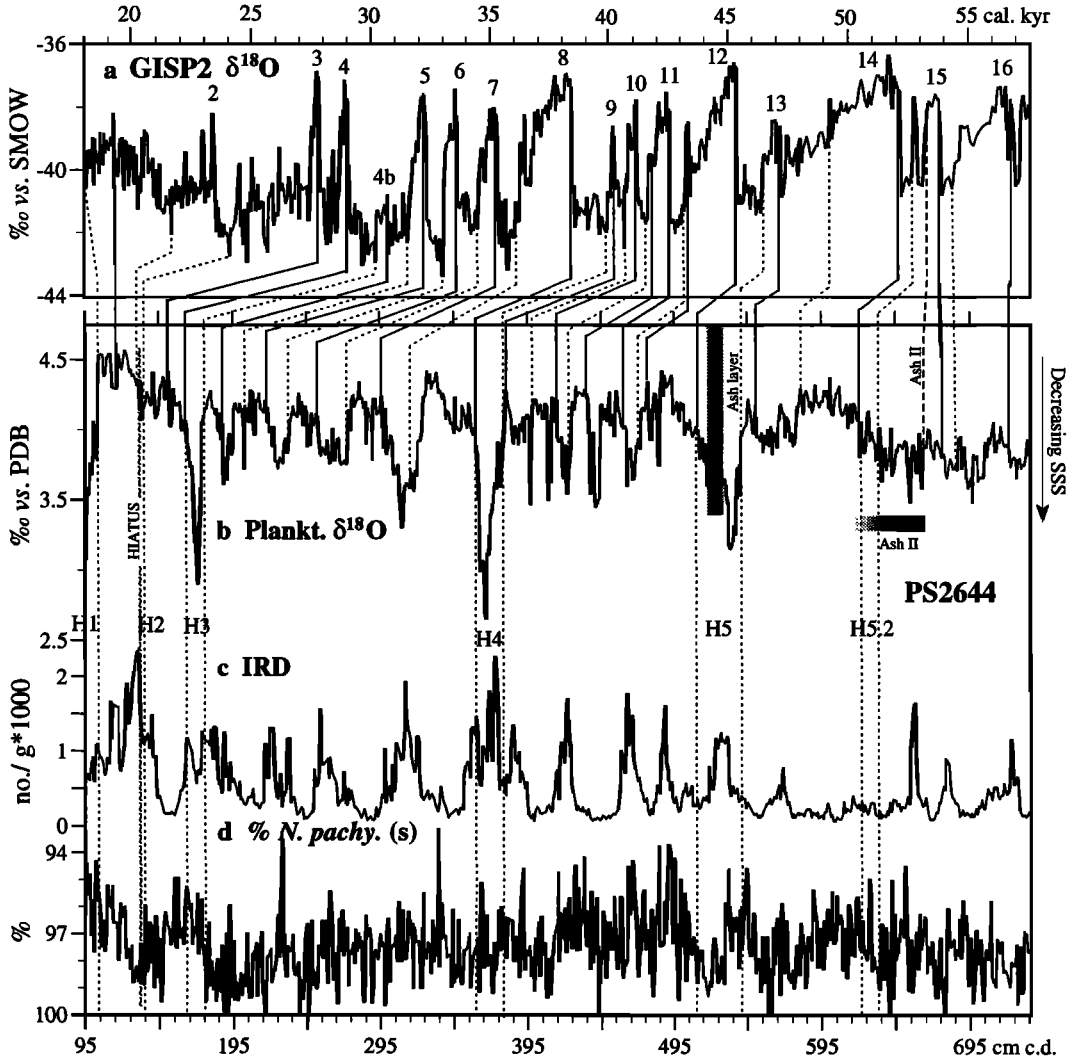

Figure 3. (a) GISP2 $\delta^{18}O$ data of temperature changes on Greenland Summit [*Grootes et al.*, 1993; *Grootes and Stuiver*, 1997] correlated to various climate records in core PS2644, plotted against composite core depth (c.d). (b) The $\delta^{18}O$ record of planktic *N. pachyderma* (s.) (Plankt. $\delta^{18}O$), a proxy of SSS oscillations/meltwater pulses, (c) concentration of ice-rafted debris (IRD >150 μm), and (d) percent *N. pachyderma* (s.) in total planktic foraminifera >150 μm (% *N. pachy.* (s)), a proxy of SST. Stippled bars mark Heinrich events H1-H5.2, as defined by extreme planktic $\delta^{18}O$ minima as proxy of meltwater events. Age correlation between GISP2 and the planktic $\delta^{18}O$ record has been roughly constrained by ~100 AMS ^{14}C datings [*Voelker et al.*, 1998] and is finally based on numerous tie points, correlating the end of meltwater signals ($\delta^{18}O$ minima) with the onset of D-O interstadials (solid lines) and the beginning of $\delta^{18}O$ meltwater signals with the onset of D-O stadials (dashed lines). Further tie points (not shown) correlate the stadial extremes with meltwater maxima.

this study. The specimens were sampled at the same intervals as the other records. Many sediment intervals, however, were devoid of this species.

Seasonal SST values were estimated from planktic foraminiferal assemblages, using the updated version 28 of SIMMAX modern analog technique transfer function [*Pflaumann et al.*, 1996] based on a maximum similarity index of species assemblages in 10 best analogs, combined with weighting the geographical distance between analog samples. This method is most suited for reconstructing SST during isotope stages 3 and 2 at the subpolar site SO82-5 because of its extensive database at high latitudes, its capability to estimate summer SST between 4° and 8°C to within 1°C, and a reduced bias to no-analog cases ([*Pflaumann et al.*, 1996] database enlarged to 916 surface samples). This equation has a multiple correlation coefficent of 0.994 for summer (August, September, and October) and 0.995 for winter (February, March, and April) SST estimates (U. Pflaumann, unpublished data, 1999).

SSS values were deduced from the $\delta^{18}O$ record of *N. pachyderma* (s.), summer SST values, and global ice volume (modified from *Duplessy et al.* [1991]). Since the summer SST at 0 m obtained by the transfer function do not necessarily correspond to the actual temperature of calcification because of metabolic effects, we obtained the effective temperature of calcification T using $T = 0.97SST_{su} - 1.92$ [*Weinelt et al.*, 1996].

Variations in global ice volume were estimated in the sense of *Labeyrie et al.* [1987] and *Vogelsang* [1990]. We nor-

malized the $\delta^{18}O$ anomaly values to 1.2‰ for the transition from the Last Glacial Maximum to the Holocene [*Fairbanks*, 1989]. The residual $\delta^{18}O$ anomaly is transformed into a salinity anomaly using a local regression slope of 1:1.79 [*Geochemical Ocean Sections Study (GEOSECS) Atlantic*, 1987], the modern $\delta^{18}O$-to-salinity relationship in the North Atlantic [*Duplessy et al.*, 1991]. In this regression the end-member of freshwater input has a $\delta^{18}O$ composition of -19.3‰ [*GEOSECS Atlantic*, 1987].

Spectral analysis was used along the lines of SPECMAP [*Imbrie et al.*, 1984, 1992] for determining the periodicities in our climatic records and deducing the relative phasing (leads and lags) within a given frequency band of 1/1460 years. We employed the program SPECTRUM [*Schulz and Stattegger*, 1997] with Welch overlapped segment averaging [*Welch*, 1967] instead of the more conventional Blackman-Tukey method because SPECTRUM is superior since it enables the analysis of unevenly spaced time series without interpolation [*Schulz and Stattegger*, 1997]. All spectral analyses were done between 46 and 22 kyr B.P. because this time span shows both the highest time resolution and the largest and most frequent variability in our paleoclimate records.

Here 71 samples were ^{14}C dated by accelerator mass spectrometry (AMS; Tables 1a and 1b). Each sample consisted of 780-2000 specimens (150-250 μm; most samples weighed between 9 and 15 mg) of *N. pachyderma* (s.) picked on their abundance highs and maxima to minimize bioturbation effects. The samples were cleaned with 99.8% ethanol in an ultrasonic bath and measured at the Kiel Leibniz Laboratory [*Nadeau et al.*, 1997]. The ^{14}C background ages were in the range of 50.0 and 53.5 kyr B.P. when ages higher than 42 kyr B.P. were measured (Table 1b; high KIA numbers (KIA is the Identification Code for Kiel (KI) AMS (A) ^{14}C laboratory)). The ages are given in ^{14}C kyr B.P. or cal kyr B.P. (calendar kilo years before present). The data sets of cores SO82-5 and PS2644 are stored in the German PANGAEA data bank (available on the World Wide Web at http://www.pangaea.de).

3. Results

The IRD concentration displays frequent and large shifts varying from 50 to 12,000 grains (>150 μm) per gram of dry sediment (Figure 2d). About 24 IRD peaks rise above the average concentration of 800 grains/g. The IRD grains consist mostly of transparent quartz and basaltic glass. Rhyolitic glass, hematite-covered quartz, feldspar (occasionally hematite-coated) (Figure 2e), volcanic rock fragments and sedimentary rock fragments, such as sandstone, siltstone, and shale, are present, while detrital carbonate and metamorphic grains are rare to absent.

The highest concentration (8500/g) of rhyolitic glass occurs at 496 cm. It comprises 71% of the nonbiogenic grains along with 6% basaltic glass and 23% other grains, such as transparent and hematite-covered quartz, sedimentary and volcanic rock fragments, and some feldspar. The transparent colorless rhyolitic glass grains are bubble walled or blocky and vesicular.

Six intervals with high concentrations (560-2200 grains/g) and percentages (6-89%) of fresh, unaltered light to dark brown basaltic glass occur at 183, 279, 354, 381, 460, and 491/496 cm near 23.6, 29.5, 37.3, 41.8, 47.2, and 48.5 ^{14}C kyr B.P., respectively (Figure 2f). These intervals also contain varying amounts of other IRD grains.

The planktic foraminiferal fauna in core SO82-5 comprise the polar, subpolar, and cosmopolitan assemblages identified in North Atlantic plankton tows [*Bé and Tolderlund*, 1971; *Hemleben et al.*, 1989]. The polar species *N. pachyderma* (s.) varies from 37 to almost 100% (Figure 4a). The subpolar species *Turborotalita quinqueloba* (0-29%), *N. pachyderma* (dextral) (0-8%), and *Globigerina bulloides* (0-32%), which dominate the surface sediment at site SO82-5 [*Lackschewitz et al.*, 1998], comprise 0-54% of the foraminiferal assemblage (Figure 4a). The cosmopolitan *Globigerinita glutinata* contributes 0-5%.

The summer SST, which closely parallel the winter SST in core SO82-5, oscillate in cycles from 1.8° to 9°C (Figures 2b, 4b, and 5), as compared to -0.6 to 4.5°C during winter. These SST cycles start with an abrupt increase in summer SST from ~4° to ~9°C, followed by a period with constant temperature or moderate cooling, and end with a rapid shift back to very cold temperatures. Accordingly, the marine SST record of several interstadials differs from the GISP2 temperature curve by displaying warm "plateaus" at D-O 14, 10, 8, 5, and 3, less at D-O 12, but not at 11, 7, and 6 (the sampling resolution of other interstadials is too low).

Except for H2 (Heinrich event 2), IRD maxima usually do not occur until the end of the cold periods, occasionally followed by a second IRD peak associated with the rapid warming of the D-O event (Figures 2b, 2d, and 5). The prolonged cold periods at 255-218 cm and 128-90 cm were punctuated by three and two IRD events, respectively (Figure 2d). The average SST estimated for the interval 119-95 cm is 4.0° ± 0.7°C in summer and 0.6° ± 0.3°C in winter.

The stable oxygen isotope values of *N. pachyderma* (s.) oscillate from 3.1 to 4.8‰ in core SO82-5 (Figure 2g). Low $\delta^{18}O$ values are generally linked to high summer SST and vice versa (compare Figures 2b and 2g). Exceptions are at 530, 221, and 90 cm, where negative excursions to 3.2, 3.4, and 3.7‰ are associated with low summer SST of 4°, 3.9°, and 3.5°C, respectively. The *N. pachyderma* (s.) $\delta^{13}C$ record displays short-term changes ranging from -0.4 to 0.5‰ (Figure 4f).

The $\delta^{18}O$ values of epibenthic *C. wuellerstorfi* vary from 4.5 to 3.1‰ (Figure 4h), while the $\delta^{13}C$ data change from 1.8 to 0.6‰ (Figure 4g). Extremely low benthic $\delta^{18}O$ data generally match very low $\delta^{13}C$ values.

4. Age Control

The chronology in core SO82-5 is based on a combination of $\delta^{18}O$ stratigraphy, 71 AMS ^{14}C dates back to 56.6 kyr B.P., ash layers, and finally, tuning the SST record (Figure 2b) to the GISP2 $\delta^{18}O$ temperature data (Figure 2a). The section covers marine isotope stage 3 and most of stage 2 based on both planktic and benthic $\delta^{18}O$ records (Figures 4d and 4h) [*Jung*, 1996; *Lackschewitz et al.*, 1998].

The AMS ^{14}C dates (Table 1 and Figure 2d) display amazingly few reversals despite the dense sampling of up to 4 cm. Large inversions mostly occur prior to 48 ^{14}C kyr B.P., which is close to the limits of AMS ^{14}C dating. Hence we

Table 1a. AMS ^{14}C Dates Measured on Monospecific Samples of the Polar Planktic Foraminifera, *Neogloboquadrina pachyderma* (s.) in Core SO82-5

Laboratory Number	Depth, cm	AMS ^{14}C Age, years	+ 1σ Error, years	- 1σ Error, years	Calendar Age in GISP2 years
KIA2721	95	15840	110	110	18005
KIA4234	110	16960	70	70	20066
KIA2722	120	18150	150	140	21633
KIA2723	128	18510	140	140	22053
KIA2724	134[a]	19730	160	150	22383
KIA4235	134[a]	19210	60	60	22383
KIA2725	138	18170	150	150	22888
KIA2726	145	19850	170	160	23259
KIA2727	152 H2[b]	20390	190	180	23746
KIA2728	156 H2[b]	20670	170	170	24060
KIA2729	160	20010	180	180	24803
KIA2730	164	21610	190	180	25256
KIA2731	168	22300	210	200	25662
KIA2732	172	22750	220	220	25935
KIA1474	176	23110	210	200	26672
KIA1475	182	23560	210	210	27114
KIA2274	187	24410	200	200	27409
KIA1798	191	24390	250	240	27521
KIA1800	195	24520	260	250	27793
KIA1801	200	25240	270	260	28069
KIA1802	206	25300	280	270	28468
KIA1476	214	25460	260	250	29030
KIA1477	221 H3[b]	26380	280	270	29692
KIA1478	226	26090	290	280	30283
KIA1479	230	26670	290	280	30514
KIA1480	234	26820	300	290	30745
KIA1481	236	26820	320	310	30903
KIA1482	240	28010	330	320	31203
KIA1483	243	28290	340	330	31331
KIA1484	245	28340	360	350	31345
KIA1485	253	28440	360	340	31459
KIA1803	259	28650	410	390	31888
KIA1804	263	28650	410	390	32123
KIA1805	274	29370	440	420	32777
KIA1806	278	29490	450	430	33319
KIA1807	283	29790	470	440	33587
KIA1808	286	30260	490	460	33627
KIA1809	289	30720	520	490	33720
KIA1810	297	30360	510	480	34130
KIA1811	304	30860	540	500	34744
KIA1812	307	31170	550	520	34972
KIA1813	311	31470	590	550	35385
KIA1814	315	31310	570	530	35571
KIA1815	320	32900	900	810	35633
KIA2275	324	33100	530	500	35861
KIA1816	328	33820	1000	890	36171
KIA2276	332	34310	610	570	36481
KIA2277	339	34070	600	560	37341
KIA2278	347 H4[b]	35860	760	690	38565
KIA2279	350 H4[b]	36090	810	730	39185
KIA2280	354	37280	900	810	40012
KIA2281	358	37000	870	790	40688
KIA2282	361	36900	860	770	40859
KIA2283	364	37590	930	840	41132
KIA2284	370	39680	1230	1070	41475

Table 1a. (continued)

Laboratory Number	Depth, cm	AMS ^{14}C Age, years	+ 1σ Error, years	- 1σ Error, years	Calendar Age in GISP2 years
KIA2285	375	40570	1370	1170	41908
KIA2286	379	41770	1680	1390	42393
KIA3825	391	43400	1420	1210	44210
KIA3826	400	43450	1460	1230	45360
KIA5448	406 H5[b]	44240	520	490	45655
KIA5449	412[a]	44630	580	540	45787
KIA3827	412[a]	41780	1150	1010	45787
KIA3828	424	46290	2170	1710	46281
KIA3829	438	49790	3330	2350	47391
KIA5450	443	48360	1020	910	47649
KIA5451	460[a]	47240	710	650	49129
KIA3830	460[a]	39660	870	780	49129
KIA4236	475	49100	920	830	50958
KIA4237	489 H5.2[b]	48520	960	860	52236
KIA4238	496	48190	790	720	53258
KIA5452	537	56210	2540	1930	56949

Ages are given in years B.P. and are corrected for an oceanic reservior effect of -400 years [*Bard*, 1988].
[a] Duplicate measurements.
[b] H2-H5.2 refer to Heinrich IRD intervals dated by AMS ^{14}C.

assume that the core has no hiatus. The interval 119-95 cm covers the Last Glacial Maximum (LGM) (18-15 ^{14}C kyr=21.5-18 cal kyr B.P. [*Sarnthein et al.*, 2000]). However, the ^{14}C ages per se do not allow the estimation of any short-term changes in sedimentation rate since both the ^{14}C reservoir effect of sea water and the atmospheric ^{14}C production have dramatically changed many times on short timescales over stage 3 [*Voelker et al.*, 1998].

In total, the outlined signals of climate change in core SO82-5, especially the SST record (Figures 2b and 4b), are extraordinarily similar to the oscillations of GISP2 air temperatures in Greenland (Figure 2a). This similarity applies to (1) the differential duration of SST variations, (2) the characteristic abrupt warming events, and (3) the range of SST shifts of 4°-7°C, which is approximately half of the various recent temperature estimates of 10°-17°C, associated with the abrupt D-O events on Greenland (calculated from 0.33 to 0.42‰/°C during stages 2-4 [*Cuffey et al.*, 1995; *Lang et al.*, 1999]). In addition, a new interstadial event found in the marine core and labeled as 4b is also identified in the GRIP and GISP ice cores (Figures 2b, 2a, and 4a). Moreover, stadial peaks in IRD concentration and SSS minima match periods with enhanced dust storms on Greenland, as documented by calcium peaks in the ice core [*Mayewski et al.*, 1994, 1997].

We converted depth to calendar age by matching the distinct warmings and coolings of SST in core SO82-5 with their temporal interstadial/stadial equivalents in the GISP2 δ^{18}O air temperature record (Figures 2b, 2a, and 5). This record was used for correlation because its age model is based on annual layer counting back to 50 cal kyr B.P., with an estimated error of ±5% [*Meese et al.*, 1994]. We used numerous tie points correlating the end of abrupt SST warmings with the onset of D-O interstadials and the beginning of SST lows with the onset of D-O stadials. Further tie points correlate the stadial extremes with SST minima. Correlation precision amounts to 1 cm, in some cases 2 cm, corresponding to 1 or 2 sampling

Table 1b. Apparent Background Ages (Blanks) and Dates of the Run While Measuring SO82-5 Samples

Laboratory Number	Background Age, years	Run Date
KIA1476 - KIA1485	45910	Feb. 14, 1997
KIA1474 - KIA1475	45270	Feb. 22, 1997
KIA1815 - KIA1816	42840	April 30, 1997
KIA1798 - KIA1814	44890	May 6, 1997
KIA2274 - KIA2286	47220	July 10, 1997
KIA2721 - KIA2732	44390	Aug. 29, 1997
KIA3825 - KIA3831	50250	Nov. 27, 1997
KIA5448 - KIA5453	53510	Aug. 12, 1998
KIA4234 - KIA4238	53510	Aug. 12, 1998

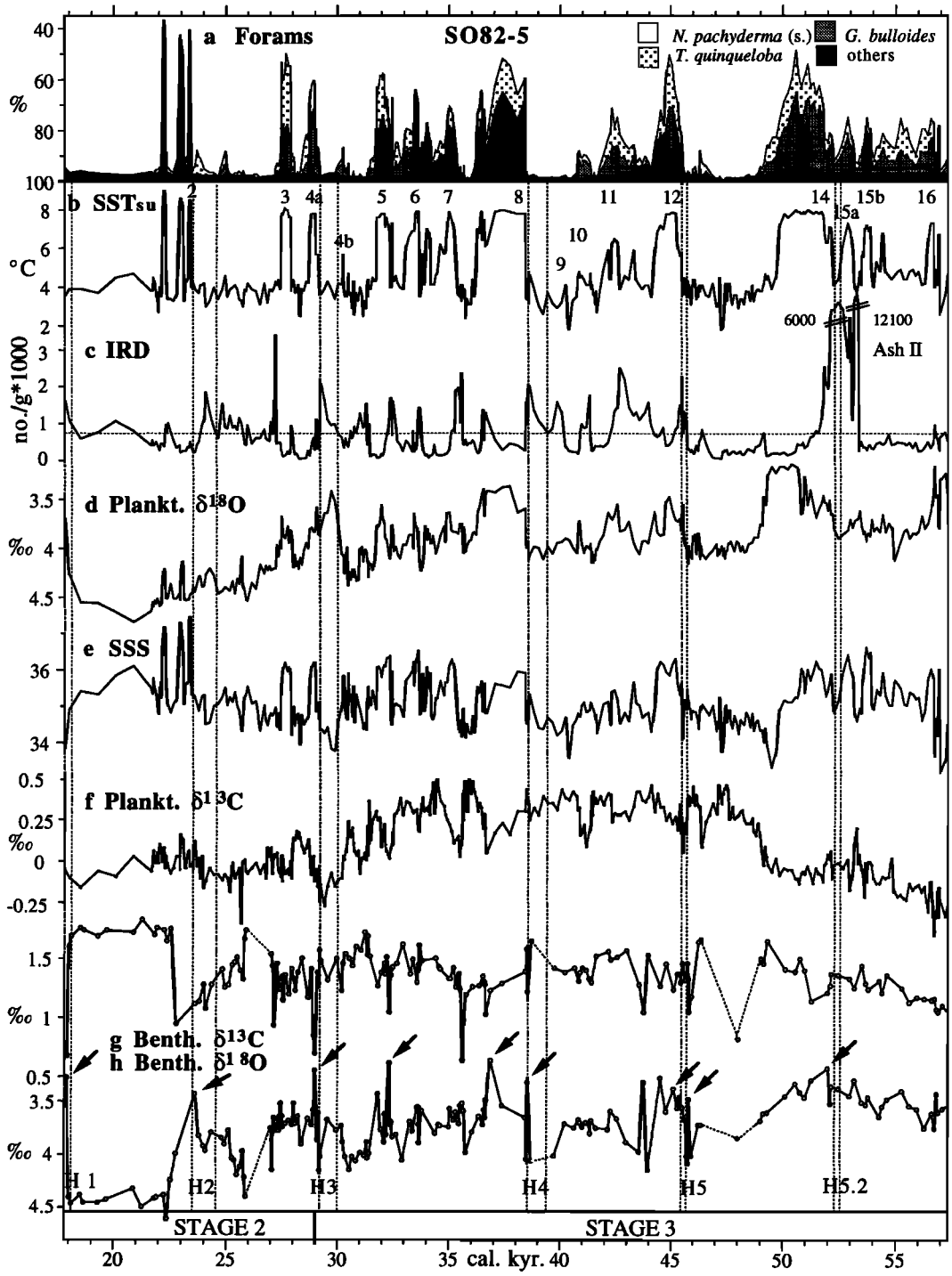

Figure 4. Core SO82-5 records of (a) percent planktic foraminifera >150 μm (Forams), (b) summer sea surface temperature (SST_{su}), (c) ice-rafted debris (IRD) concentration >150 μm, (d) $\delta^{18}O$ of *N. pachyderma* (s.) (Plankt. $\delta^{18}O$), (e) sea surface salinity (SSS) (f) $\delta^{13}C$ of *N. pachyderma* (s.) (Plankt. $\delta^{13}C$), (g) $\delta^{18}O$ and (h) $\delta^{13}C$ of epibenthic *C. wuellerstorfi* (Benth.) [*Jung.*, 1996; with additional new data from this study]. Calendar ages are based on 71 AMS ^{14}C dates and on fine-tuning the SST_{su} record to the annual layer counted GISP2 $\delta^{18}O$ timescale [*Meese et al.*, 1994; *Grootes and Stuiver*, 1997]. Numbers 2-16 refer to D-O interstadials [*Johnsen et al.*, 1992]. Sea surface salinity was estimated using a ratio of $\delta^{18}O_{water}$ to SSS of 1:1.79 [*GEOSECS Atlantic*, 1987] Horizontal dashed line and stippled bars are as in Figure 2. Arrows mark benthic $\delta^{18}O$ brine water signals.

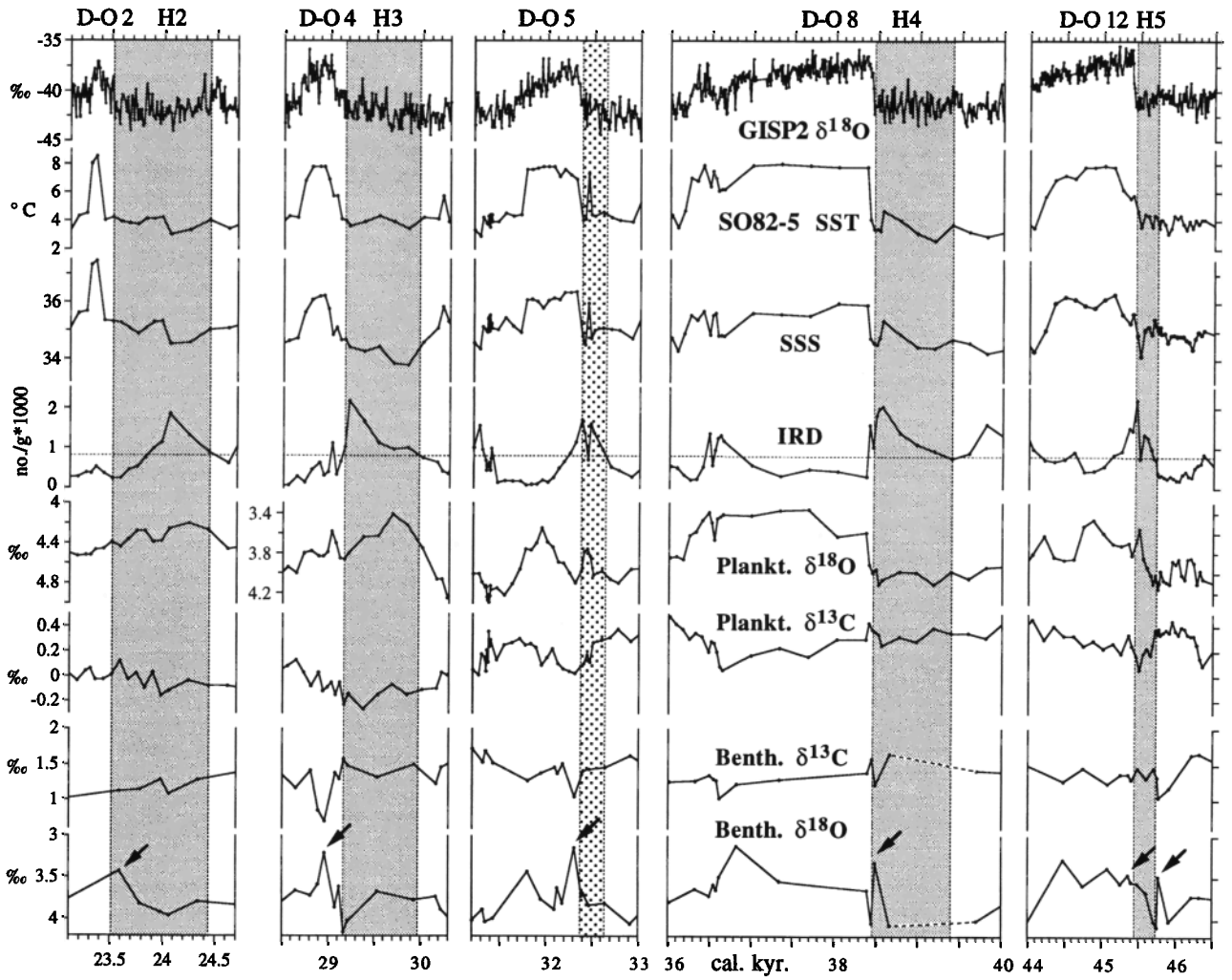

Figure 5. Ultrahigh resolution GISP2 $\delta^{18}O$ data (20 cm, [*Stuiver and Grootes*, 2000]) and SO82-5 records plotted on an expanded scale. Gray bars mark Heinrich events H2-H5. Coarsely stippled bar shows a prominent ice-rafting event prior to D-O 5. Arrows show benthic $\delta^{18}O$ brine water signals. Note scale change in planktic $\delta^{18}O$. Sea surface salinity was estimated using a ratio of $\delta^{18}O_{water}$ to SSS of 1:1.79 [*GEOSECS Atlantic*, 1987]. Benthic data are from *Jung* [1996; with additional new data in this study].

intervals, which equate to 80-160 years (Figure 5). The correlation is only tentative for the D-O 13 interstadial (Figure 2). The stadial prior to D-O event 10 was solely identified by an IRD peak.

Different from the 80-year resolution of the other proxy records, the benthic isotope record in core SO82-5 has an average resolution of ~190 years between 22 and 46 kyr B.P. and ~170 years between 27 and 37 kyr B.P. Even this record is sufficient for high-resolution phase analyses within the 1/1460-year frequency band.

Core PS2644 from north of Iceland (Figures 1 and 3; details are given in *Voelker* [1999]) shows an average resolution of 50 yr/cm, somewhat higher than in core SO82-5. The stratigraphy of core PS2644 was also tuned to GISP2 using the same technique but different parameters. Initially, the age correlation of stages 2-3 was roughly constrained by ~100 AMS ^{14}C datings [*Voelker et al.*, 1998]. Finally, it was based on numerous tie points (Figures 3a and 3b), correlating the end of meltwater signals ($\delta^{18}O$ minima which are not correlated to SST minima) with the onset of D-O interstadials in GISP2 and the beginning of $\delta^{18}O$ meltwater signals with the onset of D-O stadials because meltwater lids at this station are opposed to any warm water advection of the Irminger Current as representative of the North Atlantic heat pump. Further tie points (not shown in Figure 3) correlate the stadial extremes with meltwater maxima. The precision of this correlation to the GISP2 master record amounts to 50-100 years (1-2 sampling intervals).

Accordingly, we can compare climatic phase relationships between the two marine sites under the assumption that the end of the $\delta^{18}O$–SSS minima in core PS2644 and the onset of the SST maxima in core SO82-5 are synchronous. The ultimate error in this comparison ranges from ~80 to 250 years.

On the basis of both the IRD record and AMS ^{14}C dates we identified a few IRD events in core SO82-5 out of 24 layers with approximately equal IRD concentrations (Figure 2d), which correspond to the Heinrich events proper in the

midlatitude North Atlantic. Accordingly, H2 has an age of 20.7-20.4 ^{14}C kyr B.P. and H3 has an age of 26.4 ^{14}C kyr B.P. (Table 1 and Figure 2d). The IRD layer of H4 was constrained to 36.1-35.9 ^{14}C kyr B.P., and the IRD layer of cold stadial H5 was constrained to 44.2 ^{14}C kyr B.P. (Table 1 and Figure 2d). H5.2, which was first identified in cores from Rockall Plateau [*Sarnthein et al.*, 2000], was dated at ~48.5 ^{14}C kyr B.P. (Table 1). By and large, these ages confirm previous datings [*Andrews and Tedesco*, 1992; *Bond et al.*,1992, 1993; *Cortijo et al.*, 1997; *Elliot et al.*, 1998; *Voelker et al.*, 1998]. However, they may vary by >2000 years, age differences that can be largely attributed to local variations in the oceanic ^{14}C reservoir effect [*Sarnthein et al.*, 2000], extremes similar to the ^{14}C reservoir effect in the modern North Pacific or near Antarctica [*Stuiver and Braziunas*, 1993].

In core SO82-5, ash zone II forms a further prime stratigraphic marker horizon, culminating at 496 cm and dated at 48.2-48.5 ^{14}C kyr B.P. (Figure 2d), which is equal to 53.3 cal kyr B.P. [*Meese et al.*, 1994] estimated in the GISP2 ice core [*Zielinski et al.*, 1996, 1997]. This is younger than the age of 55 cal kyr B.P. assigned by *McManus et al.* [1998] and other previous estimates of 57.5-65 kyr B.P. [*Ruddiman and Glover*, 1972; *Fillon and Duplessy*, 1980; *Ruddiman and McIntyre*, 1984]. The final age model (Figures 4 and 5) was derived from linear interpolation between the narrow-spaced calendar age control points, chosen at the beginning and end of the abrupt terminations of stadials and their extremes, and ash zone II (compare Figure 2).

5. Discussion

5.1. IRD Sources and Transport Directions

The sedimentary records in the midlatitude North Atlantic are marked by a few major Heinrich IRD layers which *Bond et al.* [1993] tied to the major cold stadials antecedent to D-O interstadials 1, 2, 4, 12 and 17, whereas much weaker IRD events precede the other interstadials [*Bond and Lotti*, 1995]. Some stadials are even void of IRD. In contrast, 24 IRD events occur in core SO82-5 that are about equal in size and precede almost every D-O interstadial (Figures 2d and 4c). Only a thin layer is found at the end of the cold stadial prior to D-O event 12.

The numerous IRD fluctuations in core SO82-5 like those in core SU90-24 [*Elliot et al.*, 1998] from the Irminger Sea provide a detailed account of surges from the Icelandic, Greenland, and other northern ice sheets from 60 to 18 kyr B.P. (Figures 2d and 4c). An Icelandic origin of icebergs can be deduced from up to 90% fresh basaltic glass, rhyolitic glass, and volcanic rock fragments in the IRD layers and is confirmed by the chemical composition of discrete ash layers in this core [*Lackschewitz and Wallrabe-Adams*, 1997; *Haflidason et al.*, 2000].

Some icebergs reaching the Irminger Sea also originated from the Greenland and Svalbard ice sheets. Here Proterozoic and Phanerozoic red beds [*Habicht*, 1979] are potential sources for the hematite-coated quartz and feldspar which we identified in all IRD layers (Figure 2e). Actually, sediment clasts occurring in the Irminger Sea sediments may have been primarily derived from sedimentary rocks exposed along the coastal areas of central and northeastern Greenland [*Birkelund and Perch-Nielsen*, 1986]. This is in agreement with LGM maxima of sediment clasts (50-75%) in cores near Greenland and north of Iceland [*Bischof*, 1994], maxima that are much larger than in the Irminger Sea core.

In contrast to ice-rafted layers in midlatitude North Atlantic, detrital carbonate characteristic of Laurentide [*Bond et al.*, 1992, 1993; *Grousset et al.*, 1993; *Gwiazda et al.*, 1996a, b; *Bond et al.*, 1997], Labrador Sea [*Andrews and Tedesco*, 1992; *Stoner et al.*, 1996], and Arctic Sea [*Bischof*, 1994] origin was not found in core SO82-5 and neighboring cores [*Elliot et al.*, 1998; *Lackschewitz and Wallrabe-Adams*, 1997]. Hence icebergs from both Canada and the Arctic Sea hardly reached the Irminger Sea during the ice-rafting events.

Like every cool phase preceding a D-O event, Heinrich events H1-H5 also have high concentrations of IRD including hematite-stained quartz (Figure 2e). Prior to the IRD maximum of H3, a distinct planktic δ^{18}O decrease by 0.8‰ at low SST indicates a significant meltwater signal in the Irminger Sea (Figures 4d and 5). The H3 salinity anomaly is in line with the findings of *Grousset et al.* [1993] that the H3 icebergs in the whole North Atlantic and thus their major meltwater injection mainly originated from the ice sheets on Iceland and Greenland. However, it is interesting to note that the IRD of H1-H2 and H4-H5 at site SO82-5 in the Irminger Sea has the same northern origin as the H3 IRD (Figure 2d). Thus no difference either in source or in size is recognized between Heinrich and non-Heinrich ice-rafting events at this site, different from the Heinrich belt.

A northern origin also applies to most ice-rafting events in cores ODP 609 and VM 23-81 from the northeast Atlantic Heinrich belt [*Bond et al.*, 1992; *Bond and Lotti*, 1995]. Here basaltic glass initially increases in H1, H2, and H4, prior to the increase of carbonate grains [*Bond and Lotti*, 1995]. This implies that the Icelandic icebergs first reached the midlatitude North Atlantic and thus triggered the HE. The Laurentide icebergs arrived later and only contributed to the extreme HE but not to the manifold small IRD layers found in between, where detrital carbonate is rare or absent.

Frequent IRD layers also occur all over the Greenland-Iceland-Norwegian Seas [*Fronval et al.*, 1995; *Nam et al.*, 1995; *Stein et al.*, 1996; *Dreger*, 1999; *Dokken and Jansen*, 1999]. The IRD layers in our ultrahigh-resolution record from north of Iceland are especially rich in volcanic glass [*Voelker*, 1999]. Different from the SST and planktic δ^{18}O records, the IRD records were not used for tuning the core stratigraphy. However, they show a common robust periodicity of 1460 years in both the Irminger and Icelandic Seas, which share approximately the same IRD source regions (Figures 6a, 6g, 6f; [*Voelker*, 1999; *Grootes and Stuiver*, 1997]). This frequency equates to that of the GISP2 temperature record. (Note that the planktic δ^{18}O and SST estimates, which were used for tuning the stratigraphy of cores PS2644 and SO82-5, respectively, and the IRD counts provide statistically independent records which, in principle, contain different and/or common periodicities. The latter may be "phase locked" only due to external climatic forcing.)

This dominant 1460-year period reflects the pace of some kind of internal instability common to the ice sheets on Iceland and Greenland, discharging icebergs into the East Greenland

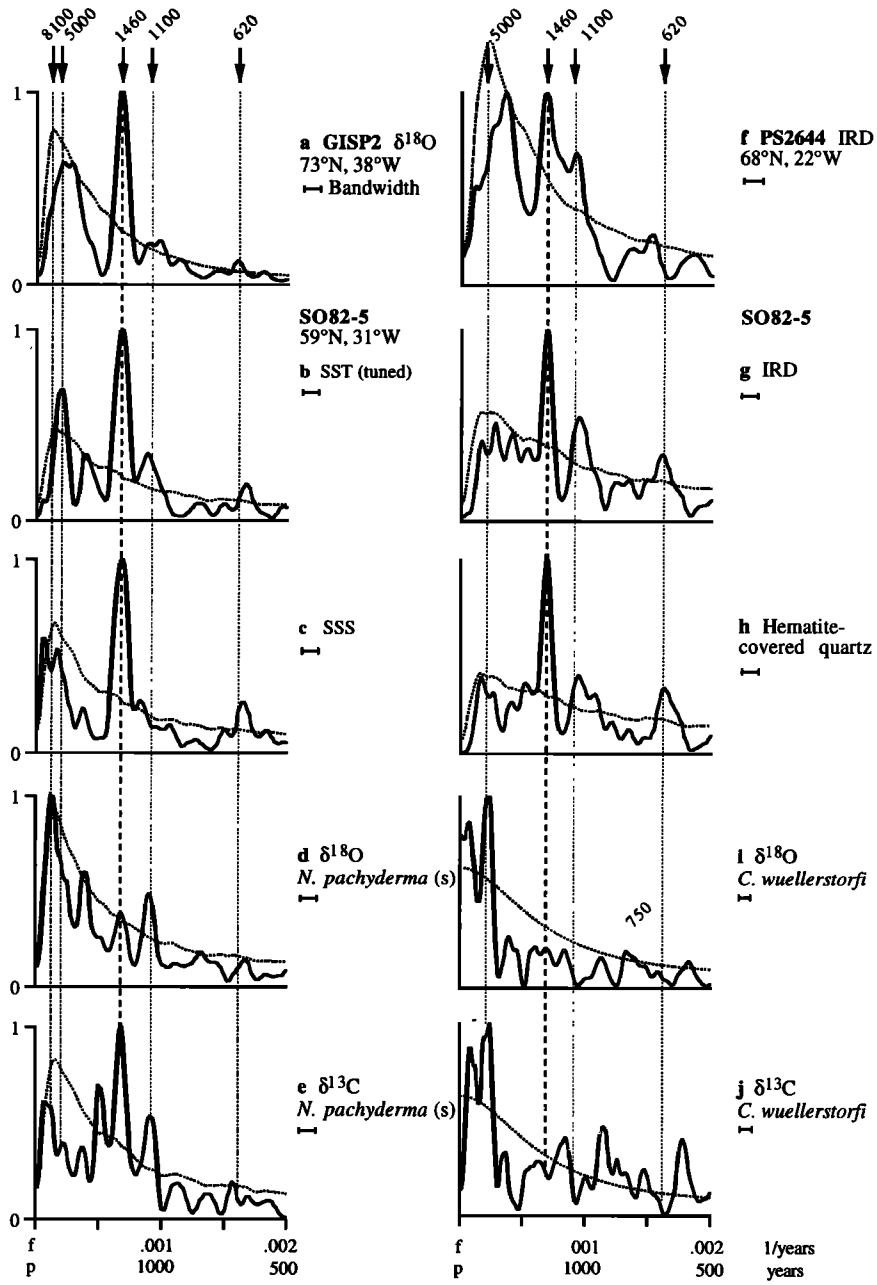

Figure 6. Power spectra, normalized to the highest peak, covering the past 46-22 kyr, obtained for (a) GISP2 $\delta^{18}O$ data and core SO82-5 data of (b) summer sea-surface temperature (tuned), (c) salinity, (d) $\delta^{18}O$ and (e) $\delta^{13}C$ of *N pachyderma* (s), ice-rafted debris concentration in cores (f) PS2644 and (g) SO82-5, (h) hematite-covered quartz concentration, and (i) $\delta^{18}O$ and (j) $\delta^{13}C$ of *C wuellerstorfi* Power spectra were calculated with SPECTRUM [*Schulz and Stattegger*, 1997] and dotted 80% confidence line was estimated according to the Redfit program (M. Schulz, personal communication, 2000; M. Schulz and M. Mudelsee, manuscipt in preparation, 2000) The 1460-yr D-O periodicity is prominent in most records. Other salient periodicities are 8100, 5000-4300, ~1100, and ~620 years.

Current. Likewise, several other paleorecords with multidecadal to centennial time resolution from the subpolar North Atlantic [*Bond and Lotti*, 1995] and Norwegian Seas [*Dreger*, 1999; *Dokken and Jansen*, 1999] are governed by the ~1500-year signal of D-O cycles. The same holds true for the magnetic susceptibility data of deepwater circulation in the Irminger Sea [*Moros et al.*, 1997], surface and deepwater proxy records 500-340 kyr B.P. [*Oppo et al.*, 1998], and GISP2 Ca record of dust supply [*Mayewski et al.*, 1997]. In addition, many records reflect a minor but also persistent periodicity of ~1100 years, which *Heusser and Sirocko* [1997] ascribed to El Nino-Southern Oscillation (ENSO) forcings.

In contrast, the large Laurentide ice sheet surged massively only every 5-10 kyr. However, these short and long IRD periodicities may be linked since the initial phase of each HE in the midlatitude North Atlantic was marked by a discharge

of basaltic glass from Iceland [*Bond and Lotti*, 1995; *Elliot et al.*, 1998]. Accordingly, IRD records from the northwestern Atlantic and the Heinrich belt reflect differential dynamics of the various ice sheets surrounding the northern North Atlantic, in harmony with the low-resolution records of *Dowdeswell et al.* [1999].

On the basis of the dispersal of hematite-covered quartz (Figure 2e) and feldspar from Greenland and of basaltic glass from Iceland (Figure 2f), icebergs from east Greenland were transported across the narrow Denmark Strait. However, within the 1460-year cycle the IRD culminated in the Icelandic Sea core 155 years prior to the IRD peak and 195 years prior to the hematite quartz peak in core SO82-5 (Figure 7). High coherencies between the cross-correlated parameters show that these phase lags are significant (Table 2 and Figure 8). Hence the icebergs were initially jammed to the north of the Denmark Strait and passed into the Irminger Sea only after significant iceberg melt and size reduction. South of the strait, these icebergs were joined by more numerous icebergs originating from southern Iceland drifting in circles across the Irminger Sea, where they partially melted. A few of them reached the North Atlantic Drift in midlatitude North Atlantic, the "Heinrich track", finally melting off western Ireland. Likewise, the areal distribution of ash zone II in the North Atlantic [*Ruddiman and Glover*, 1972] demonstrates that the volcanic ash erupted onto ice near Iceland was transported by ice rafting in a counterclockwise flow across the Irminger Sea to the south and then to the east near the onset of a stadial prior to D-O event 15a, in harmony with a transport model of *Schäfer-Neth and Stattegger* [1998].

5.2. Sea Surface Hydrology

On the basis of the sediment records in core SO82-5 (Figures 2, 4, and 5) the sea surface circulation in the Irminger Sea changed frequently and rapidly between three major modes over the time span 60-18 kyr B.P. Today, the site area is bathed by warm, saline waters of the Irminger Current, a northwestern branch of the North Atlantic Drift, with hardly any icebergs reaching this region and average SST near 11°C in summer and 9°C in winter [*Levitus*, 1982]. About 500 km northwest of the site (Figure 1), the southern limit of the East Greenland Current marks the polar front [*Krauss*, 1986].

During stage 3/2 interstadials the surface water circulation was probably similar to the present. There was an active thermohaline heat advection of the Irminger Current, as indicated by the high summer SST averaging 8°C and reaching 9.4°C, and high SSS (>36) in core SO82-5 (Figures 4b and 4e). High *N. pachyderma* $\delta^{13}C$ values imply well-ventilated surface water, and low concentrations of IRD grains indicate minimal iceberg influx in the Irminger Sea (Figure 4f and 4c).

During stage-3 stadials, however, marked ice-rafting events suggest that the polar front shifted progressively southward, with the East Greenland Current possibly expanded and diverted to the south. This is inferred from the icebergs and cold freshwater originating from east Greenland and the Denmark Strait, which cannot reach site SO82-5 upstream and across the warm and salt-enriched Irminger Current as it flows today. Accordingly, the thermohaline heat advection of the Irminger Current ceased during stage-3 stadials, and the Irminger Sea was covered by low-salinity water as soon as the summer SST dropped to 4°C or less at site SO82-5 (Figure 4b and 4e), as it is off east Greenland today. In the 1460-year cycle the SSS minimum due to meltwater injections already occurred 220 years prior to the maximum ice rafting (Figure 7).

Highly coherent phase relationships (Figures 7 and 8) demonstrate that gradual iceberg melt in the cold ocean has led to a maximum stratification of surface water in the Irminger Sea only 310 years after peak ice rafting. The stratification is revealed by a reduction in surface water ventilation as depicted by prominent minima in planktic $\delta^{13}C$ (Figure 4f) [*Sarnthein et al.*, 1995]. Probably, the same reduction occurred in the whole northwestern Atlantic surrounding the subpolar gyre. Also, the meltwater lid of H4 is reflected by a prominent

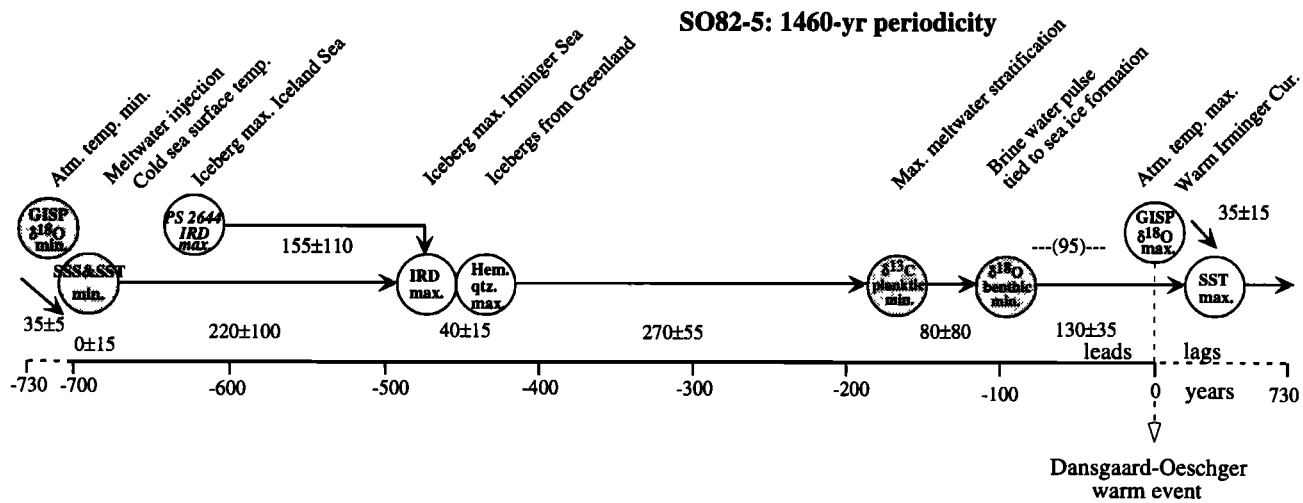

Figure 7. Average temporal leads (internal response time and error range in years) of meltwater, brine water, and ice-rafting events at site SO82-5 in the Irminger Sea versus maximum coolings and warmings in the Irminger Current and on Greenland Summit in a 1460-year D-O cycle. IRD maximum in Icelandic Sea core PS2644 leads the IRD peak in core SO82-5 by 155 years. The brine water peak leads the air temperature maximum over Greenland by 95 years.

Table 2. Phase Relationships of Cross-Correlated Variables at the 1/1460-Year Frequency Band

Time Series	Phase Angle, deg	Error, deg	Lag, years	Error, years	Bandwidth	Coherency	False Alarm (α=0.2)
$GISP_{min}/SSS_{min}$	8.7	1.7	35	5	1.31x10-4	0.99	0.66
SSS_{min}/SST_{min}	0.6	4.0	0	15	1.31x10-4	0.99	0.66
SST_{min}/IRD_{max}	55.1	24.5	220	100	1.64x10-4	0.58	0.51
IRD_{max}(PS2644)/IRD_{max}(SO82-5)	38 9	27.2	155	110	1.64x10-4	0 53	0.51
IRD_{max}/Hem_{max}	9.6	4.0	40	15	1.31x10-4	0.99	0 66
Hem_{max}/Plankt. $\delta^{13}C_{min}$	66.3	13.2	270	55	1.31x10-4	0.86	0.66
IRD_{max}/Plankt. $\delta^{13}C_{min}$	75.9	16.2	310	65	1.31x10-4	0.98	0.66
Plankt. $\delta^{13}C_{min}$/Benth. $\delta^{18}O_{min}$	19.4	19 0	80	80	1.31x10-4	0.82	0.66
Benth. $\delta^{18}O_{min}/SST_{max}$	32.5	8.7	130	35	1.31x10-4	0.93	0.66
$GISP_{max}/SST_{max}$	9.0	3 6	35	15	1.31x10-4	0.99	0 66

Coherency between two time series was calculated at 80% confidence interval. Coherency value higher than the false alarm level is considered significant. Positive angles mean that the first variable leads the second one and vice versa. Lags in years are rounded to 5. Core PS2644 was recovered north of Iceland (Figure 1) GISP, Greenland Ice Sheet Project 2 GISP2 $\delta^{18}O$ [*Grootes and Stuiver,* 1997]; SSS, sea surface salinity; SST, sea surface temperature, IRD, ice-rafted debris concentration; Hem, hematite-covered quartz concentration; Plankt. $\delta^{13}C$, *N. pachyderma* (s.) $\delta^{13}C$; Benth. $\delta^{18}O$, *C. wuellerstorfi* $\delta^{18}O$.

local increase in planktic ^{14}C reservoir ages up to >2000 years [*Sarnthein et al.*, 2000].

In contrast, an enhanced paleo-Irminger Current probably entered the Icelandic Sea during the LGM [*Sarnthein et al.*, 1995]. These authors attributed this current pattern to a low-salinity lid around the Rockall Plateau west of Ireland due to the melting of numerous Laurentide icebergs, thereby diverting the advection of warm water toward Iceland and the Denmark Strait. The low concentrations of Icelandic glass in the LGM sediments of Irminger Sea cores [*Elliot et al.*, 1998] are in support of a strong paleo-Irminger Current.

6. Origin of D-O Cycles Deduced From The Phasing of IRD, Meltwater, and Benthic $\delta^{18}O/\delta^{13}O$ Signals

The majority of the IRD peaks in core SO82-5 occur near the end of low-SST stadials (Figures 4 and 5). *Bond and Lotti* [1995] reported a similar late timing for the Heinrich and other IRD layers in the midlatitude North Atlantic, only occurring after the onset of extreme cooling. These data spuriously suggest that the surge-like events producing icebergs from ice sheets on Greenland, Svalbard, and Iceland only developed during but not prior to these cold periods. Along the East Greenland margin, several major outlet glaciers up to 850 m thick can pass internal thresholds, rapidly advance near sea level to a maximum seaward position, and result in massive calving [*Funder et al.*, 1998].

On the basis of our new SSS records of cores SO82-5 (Figures 4e and 5) and PS2644 (Figure 3b) we now can much better assess the timing and potential implications of those glacier surges for D-O cycles: Their meltwater injections are necessarily tied to the East Greenland Current passing the Denmark Strait and hence can be directly traced from the core sites upstream, up to the crucial regions of North Atlantic deepwater convection in the Greenland, Icelandic, and Irminger-Labrador Seas (Figure 1), which dominantly control the turnoff of the North Atlantic THC [*Hopkins*, 1991]. According to the models of *Paillard and Labeyrie* [1994] and *Rahmstorf* [1995], a THC shutdown, more or less extreme, has triggered the onset of most D-O stadials. Indeed, a major SSS reduction by as much as 1.5-3.5‰ directly paralleled each decline in SST and GISP2 temperatures. This large salinity shift is limited to the East Greenland Current region and does not occur in the Norwegian Current along with non-Heinrich stadials [*Voelker*, 1999]. This suggests a direct meltwater forcing of the coolings north and south of Iceland, at sites PS2644 and SO82-5 (Figures 3, 4, and 7), rather than a moderate general freshening due to THC shutdown. Vice versa, high SST and SSS persisted in core SO82-5 during interstadials when the Irminger Current passed close to this site and induced a high heat flux to the north.

In conclusion, meltwater injections and the onset of D-O stadials preceded the supply of IRD at site SO82-5 by several hundred years (Figure 7), in the case of the meltwater extreme at H3 by ~400 years (Figure 5). SSS decreased to a lesser extent at H4 and H5 and prior to D-O 5 and 6, in part, because it had already been at a low level during preceding smaller D-O cycles; nevertheless, the SSS always decreased prior to the IRD maximum (Figures 4 and 5).

If not measuring artifacts, the leads of the SSS minima versus peaks in IRD deposition may be explained by (1) clean ice melting antecedent to surging of dirty land ice in the source area (D.R. MacAyeal, personal communication, 1998) and/or (2) meltwater injections linked to surges from Greenland and other northern regions. On the other hand, we do not expect any major fluvial runoff pulses from the continents encompassing the Nordic Seas and Arctic Ocean during stages 3-2, except for the Younger Dryas event [*R.F. Spielhagen et al.*, submitted manuscript, 2000]. On the basis of Figure 7 and the consistent IRD composition at sites PS2644 and SO82-5 the meltwater pulses led the IRD deposition north of Iceland by 65 years. Icebergs reached the Irminger Sea via the East Greenland Current only 155 years later (Figure 7). Thus we infer that icebergs thicker than 400-600 m were initially jammed for several decades in the deep fjords of east Greenland and again for a few centuries in the Denmark Strait until they were reduced in size, with ongoing meltwater production.

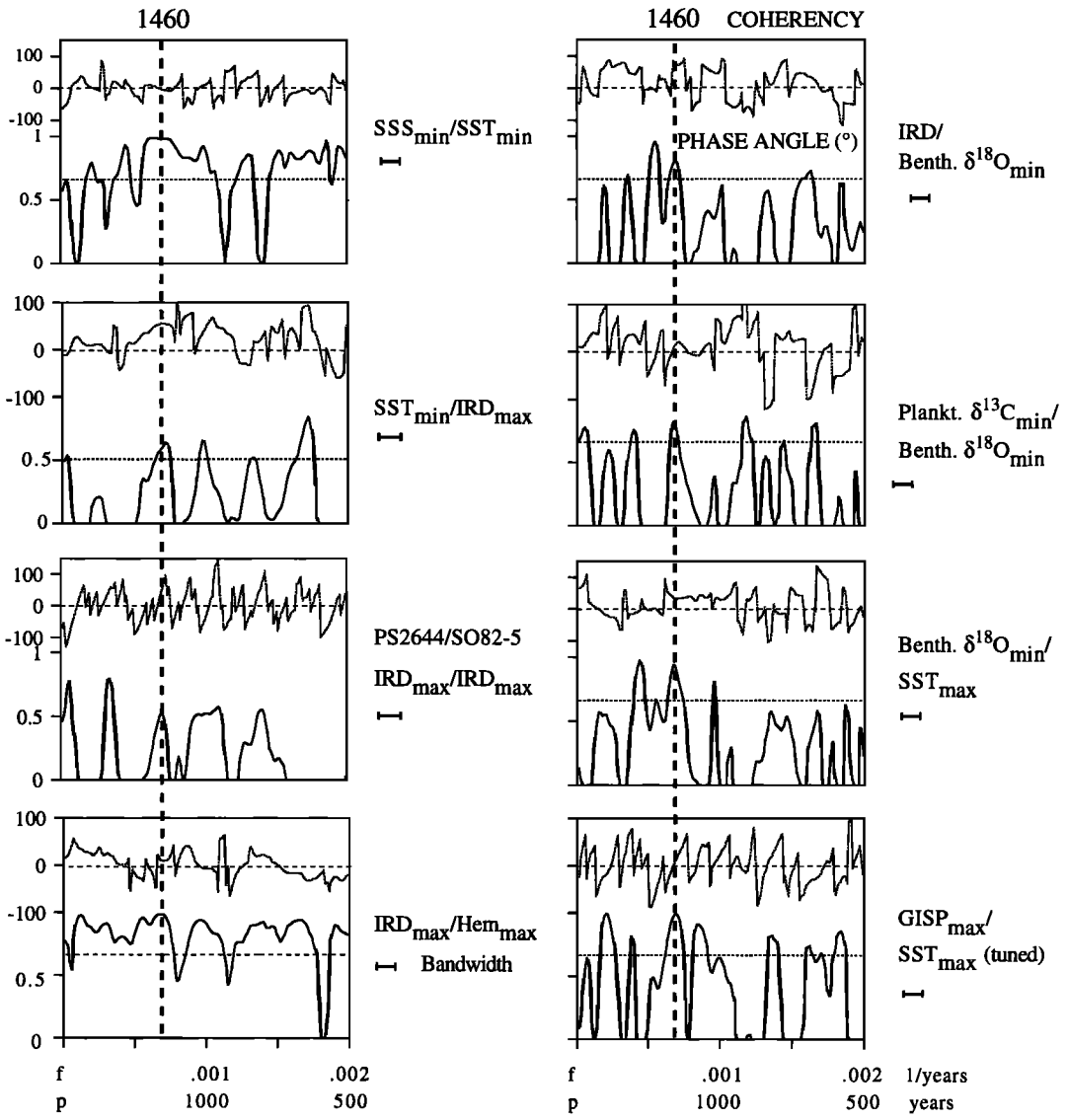

Figure 8. Coherency and phase angle (degrees) between each two time series. Positive angles indicate that the first variable leads the second one and vice versa. If minima (min) of proxies were tested for coherency, the values were multiplied by −1. Coarsely dashed horizontal line delineates the zero degree phase angle. Thin dashed horizontal line indicates a non zero coherency at 80% confidence level. Coherency values higher than this false alarm level are considered significant A 1460-year period is shown by vertical dashed line. Abbreviations are as in Table 2.

On the other hand, initial pulses of pure clean ice melting may have partially induced the D-O coolings. After a few decades, these pulses were succeeded by D-O surges of icebergs rich in IRD from the Greenland continental ice sheet, inducing the huge short-lasting changes in debris flux both to the north and south of Iceland (Figures 3 and 4). Once the Greenland ice was not held back by the "clean" shelf ice, it was probably driven by its own purely internal dynamics tied to the rugged bottom topography and thereby formed the pacemaker of the robust 1460-year period. This model of an ever recurring major initial injection of clean shelf ice and dirty iceberg meltwater to the Irminger and Labrador Seas should be traced more thoroughly, searching for decadal-scale records in front of various fjord sites along the western (and northern) margin of the Nordic Seas.

These results differ from an alternative concept of *Cane* [1998]. He proposed that the cycles may arise from an internal ENSO-like oscillation within the tropical Pacific, triggering the changes in global THC. This model is appealing because 1500 years may come close to the global turnover time of the ocean. However, it is difficult to find a process explaining how this tropical oscillation may have induced a major melting of east Greenland continental and shelf ice coeval with abrupt climatic cooling. Likewise, the model, which proposes that shutting down the THC may cause the freshening of surface water and general cooling, cannot explain the major iceberg

pulses leading to IRD layers which are very prominent to the north of Iceland at almost constant low SST (Figure 3d) and reach as far south as the mid-Atlantic ridge at 59°N (Figure 4).

The Heinrich events, which clearly lagged the onset of D-O stadials by a few centuries or so (as reflected by the advection of IRD from the north [*Bond and Lotti,* 1995]) and of meltwater; Figures 3-5) were probably simply induced by an initial slight sea level rise tied to the significant D-O freshwater influx. We assume that the rise proceeded from the initial D-O surges from east Greenland and Iceland and occasionally triggered, after a few hundred years, the much larger surges from the major Laurentian ice sheet near sea level, which possibly had a sort of internal time constant for its surges of ~7.2 kyr [*Sarnthein et al.*, 2000].

The forcing mechanisms of the most spectacular event of D-O cycles, the origin of the abrupt jumps to warm climate, may get clearer when closely inspecting the short-lasting epibenthic $\delta^{18}O$ ($\Delta\delta$ 0.5-1.3‰) and $\delta^{13}C$ ($\Delta\delta$ 0.3-1.0‰) minima which reach well beyond the average in core SO82-5 (much more pronounced change of 2‰ at H1 event in core PS2644 [*Voelker,* 1999]). Their D-O periodicity is one half of 1460, equal to ~750 years (Figure 6). The minima generally lag the IRD peaks of six D-O stadials by an average of ~390 years (Figure 7; also compare Figures 4 and 5). Because of the moderate sampling resolution we only found minor changes in benthic $\delta^{18}O$ and $\delta^{13}C$ at the other D-O stadials in core SO82-5. However, in a benthic stable isotope transect across Rockall Plateau from 1500 to 3800 m water depth, $\delta^{13}C$ fluctuated significantly along with most D-O cycles and $\delta^{18}O$ decreased by 0.5-1.0‰ along with H1, H3-H5, and various other stadials over the complete depth range [*Jung*, 1996; *Sarnthein et al.*, 2000]. A similar benthic $\delta^{18}O$ decrease went along with the D-O stadials in the northern Faeroe Channel (core ENAM 93-21), here in phase with the planktic $\delta^{18}O$ minima that display the meltwater events [*Rasmussen et al.*, 1996; *Vidal et al.*, 1998]. *Veum et al.* [1992] first explained these benthic $\delta^{18}O$ minima as brine water spikes, recording preferential sea ice formation in salt-depleted meltwater lids. This process strongly increases the density but minimally affects the oxygen isotope composition of brine water [*Craig and Gordon*, 1965], which preserves the low $\delta^{18}O$ values of low-salinity water. The coeval benthic $\delta^{13}C$ minima reveal an admixture of the brine water to pools of poorly ventilated deep water originating from the Southern Ocean and rising up to <2000 m depth [*Sarnthein et al.*, 1994; *Vidal et al.*, 1998].

In summary, these records from the northwestern Atlantic suggest that brinewater injections were characteristic of the end of all Heinrich and many other D-O stadials. The brines resulted from enhanced (seasonal) sea ice formation in the meltwater pools of vast iceberg armadas which finally spread, while melting, across the whole northwestern Atlantic and ended in a widespread thin meltwater lid, however, generally less intense than in the early stadial at site SO82-5. Our findings clearly differ from the records near Faeroe, where brines have occurred much earlier, almost instantaneously with the onset of the stadials according to the time correlation proposed by *Dokken and Jansen* [1999].

At site SO82-5 the distinct brine water pulses lead the subsequent abrupt D-O warmings by only <95 years (Figure 7). This short interval already comes close to the age uncertainty in this record (80 years for planktic and 170-190 years for benthic data). In view of this immediate succession, we consider intensive brine formation in the northwestern North Atlantic as the crucial process in forcing the actual D-O events: It may have finally entrained warm surface water from the subtropics, thereby triggering the enigmatic sudden reinvigoration of the salinity conveyor belt and, consequently, the rapid warming, the "SST jump" characteristic of the D-O events, which implied a general recovery of Northern Hemisphere climate.

At these jumps the multidecadal to centennial-scale resolution records of core SO82-5 display a further feature of D-O cycles yet undescribed. At least, the abrupt warmings linked to D-O events 4, 12, and 14 were each composed of two distinct steps (Figures 2 and 5). For example, subsequent to the IRD maximum near the end of H3, H5, and H5.2, the SST increased abruptly, possibly followed by another mini Younger Dryas style cold spell or temperature plateau near 6°C (Figure 5; shown by a sequence of 2, 3, and 4 proxy values, respectively). These potential climatic setbacks and plateaus, in part, may exceed noise because they generally match a distinct minor IRD maximum, indicating a renewed short-term iceberg advection over ~80-250 years. Only later, the SST rose to a maximum of ~8°C characterizing the D-O 4, 12 and 14 interstadials. On the basis of this combined evidence, several of the secondary SST and IRD events may be real and result from special small ice calving events in the course of rapid destadial warming.

Our model on the genesis of D-O cycles leaves a potential problem unsolved since the cycles also persist through interglacial times with low ice volume [*Kennett and Ingram*, 1995; *Sirocko et al.*, 1996; *Bond et al.*, 1997; *Schulz et al.*, 1998; *Bianchi and McCave*, 1999; *Hendy and Kennett*, 1999; *Ninnemann et al.*, 1999; *Wang et al.*, 1999]. Here they are yet hard to explain since it may prove difficult to verify the two trigger mechanisms, now identified in the Northwest Atlantic only for stages with glacial and transitional climate, (1) the meltwater incursions of east Greenland origin for the cooling and (2) sea ice triggered brine water formation for the abrupt entrainment of subtropical surface water, causing the "final" D-O warming event. Indeed, *Bond et al.* [1997] presented evidence of minor Holocene ice rafting which may have implied meltwater injections, and *Bianchi and McCave* [1999] showed variations in intensity of THC, possibly correlated to the injections. However, this line of evidence is still insufficient for uncovering the forcing mechanisms of Holocene D-O cycles.

7. Conclusions: North Atlantic Control of D-O Cycles

1. Most paleoceanographic records in cores SO82-5 and PS2644 follow a dominant D-O periodicity of 1460 years for the interval 46-22 kyr B.P., besides a less pronounced periodicity of 1100 years (Figure 6). With regard to SST in SO82-5 and planktic $\delta^{18}O$ in PS2644 the 1460-year cyclicity is the result of tuning to the periodicity found in the GISP2 $\delta^{18}O$ record [*Grootes and Stuiver*, 1997]. It is most important that the same robust cyclicity also governs most of the untuned paleoclimatic records from the Irminger and Icelandic Seas,

such as that of IRD, meltwater injections, and surface and deepwater ventilation. Moreover, several other paleorecords with multidecadal to centennial time resolution from the subpolar North Atlantic, Icelandic, and Norwegian Seas are governed by the same ~1500-year signal of D-O cycles.

2. Thus most different processes at different locations in the northern North Atlantic and the atmosphere above Greenland Summit have behaved as a coupled system, such as today, with a joint master periodicity. The potential origin of the D-O cycles, the meltwater injections were traced by means of the (delayed) hematite IRD input from site SO82-5 southwest of Iceland back to east Greenland and to the northwestern Nordic Seas, upstream from the east Greenland Current. Moreover, we used the phase leads and lags amongst the various system components in the 1/1460-year frequency band.

3. Several coolings of the sea surface in the Irminger Sea are abrupt, compared to the apparent gradual cooling of the air over Greenland as indicated by $\delta^{18}O$. The coolings in the Irminger Sea obviously result from significant reductions in SSS which precisely run in phase (Figure 7). The SSS minima depict major meltwater injections, presumably from east Greenland or farther north, that were advected along with the East Greenland Current right to the crucial sites of deepwater convection in the northwest Atlantic. Thus we conclude that surge-like outflows from the east Greenland ice sheet possibly linked to some sort of internal ice dynamics may be the pacemaker of the turnoffs of the Atlantic THC and heat advection to the high north, i.e., the onset of D-O stadials, in harmony with the models of *MacAyeal* [1993a, b] and *Rahmstorf* [1995]. Our results are opposed to an alternative concept of *Cane* [1998] proposing that the 1500-year cycle may arise from an internal ENSO-like oscillation within the tropical Pacific, triggering changes in global THC.

4. The deposition of IRD from east Greenland and Iceland lagged the initial meltwater injections by ~65 years in the Icelandic Sea and 220-260 years in the Irminger Sea (Figure 7). This suggests that the icebergs from Greenland were first jammed in the narrow Denmark Strait and only passed after some size reduction and loss of IRD, linked to partial melt. The discharge of IRD from east Canada during Heinrich events, in turn, further lagged the ice rafting from North Atlantic sources [*Bond and Lotti*, 1995]. This lag suggests that a slight sea level rise emanating from East Greenland surges finally released the surges from the Laurentian ice sheet, however, only every 5-9 kyr because of slower internal ice dynamics.

5. Continued iceberg melt led to a planktic $\delta^{13}C$ minimum. This is a record of maximum surface water stratification in the Irminger Sea, which occurred about 310 years after maximum IRD deposition. Extensive sea ice formation at reduced SSS during the stadials finally induced a conspicuous brine water convection which is recorded in benthic $\delta^{18}O$ minima all over the deep North Atlantic. Because of the short phase lead of ~95 years to global warming we surmise that this brine formation finally entrained abundant warm surface water from the subtropical North Atlantic and thereby led to an abrupt turn-on of the Atlantic THC, thus causing the spectacular D-O events of warming.

6. Our model on the genesis of D-O cycles cannot fully explain how D-O cycles can persist through Holocene and Eemian interglacial times when glaciers retreated far back into the Greenland fjords. In these stages, the various lines of evidence concerning the advection of IRD and the variability of THC are still insufficient for uncovering the forcing mechanisms.

Acknowledgments. We thank Markus Pepping, Michael Kelm, Boris Ludz, and the other students who carefully processed the samples and picked foraminifera for AMS and isotope measurements. The discussions with Klas S. Lackschewitz and Matthias Moros were very helpful. We are greatly indebted to Michael Schulz for his assistance in spectral analysis. We thank Dirk Lein, Ute Schuldt and C. Samtleben of the Scanning Electron Microscope Laboratory in the Inst. of Geosciences, Kiel Univ. for the ~250 micrographs of planktic foraminifera which enabled a better identification of the species under the binocular microscope. We are grateful to the reviewers for their valuable comments which helped improve the manuscript. This IMAGES-related study was funded by the Human Capital and Mobility program of the European Union (Project No. ENV4-CT95-0131), and the German National Climate Project funded the AMS ^{14}C datings.

References

Alley, R B , and D R MacAyeal, Ice-rafted debris associated with binge/purge oscillations of the Laurentide Ice Sheet, *Paleoceanography, 9*(4), 503-511, 1994

Alley, R , G Bond, J Chappellaz, C Clapperton, A Del Genio, L Keigwin, and D Peteet, Global Younger Dryas?, *Eos Trans. AGU, 74*(50), 587-589, 1993

Andrews, J T , and K Tedesco, Detrital carbonate-rich sediments, northwestern Labrador Sea Implications for ice-sheet dynamics and iceberg rafting (Heinrich) events in the North Atlantic, *Geology, 20*, 1087-1090, 1992

Bard, E , Correction of accelerator mass spectrometry ^{14}C ages measured in planktonic foraminifera: Paleoceanographic implications, *Paleoceanography, 3*(6), 635-645, 1988.

Bé, A W H., and D S. Tolderlund, Distribution and ecology of living planktonic foraminifera in surface waters of the Atlantic and Indian Oceans, in *The Micropaleontology of the Oceans*, edited by B M. Funnel and W.R. Riedel, pp. 105-149, Cambridge Univ Press, New York, 1971.

Bianchi, G , and N. McCave, Holocene periodicity in North Atlantic climate and deep-ocean flow south of Iceland, *Nature, 397*, 515-517, 1999

Birkelund, T., and K. Perch-Nielsen, Late Paleozoic-Mesozoic evolution of central east Greenland, in *Geology of Greenland*, edited by A Escher and W.S Watt, pp 307-340, Grönland Geol. Unders., Copenhagen, 1986.

Bischof, J.F., The decay of the Barents ice sheet as documented in Nordic seas ice-rafted debris, *Mar. Geol., 117*, 35-55, 1994.

Bond, G C., and R Lotti, Iceberg discharges into the North Atlantic on millennial time scales during the last glaciation, *Science, 267*, 1005-1010, 1995

Bond, G., et al , Evidence for massive discharges of icebergs into the North Atlantic ocean during the last glacial period, *Nature, 360*, 245-249, 1992

Bond, G., W. Broecker, S. Johnsen, J. McManus, L Labeyrie, J. Jouzel, and G. Bonani, Correlations between climate records from North Atlantic sediments and Greenland ice, *Nature, 365(9)*, 143-147, 1993.

Bond, G , W Showers, M Cheseby, R. Lotti, P Almasi, P deMenocal, P Priore, H Cullen, I Hajdas, and G Bonani, A pervasive millenial-scale cycle in North Atlantic Holocene and glacial climates, *Science, 278* 1257-1266, 1997.

Broecker, W.S , Massive iceberg discharges as triggers for global climate change, *Nature, 372*, 421-424, 1994

Broecker, W S., G Bond, M. Klas, G Bonani, and W Wolfli, A salt oscillator in the glacial Atlantic? The concept, *Paleoceanography, 5*(4), 469-477, 1990

Broecker, W , G Bond, M Klas, D. Clark, and J McManus, Origin of the northern Atlantic's Heinrich events, *Clim. Dyn., 6*, 265-273, 1992.

Cane, M A , A role for the tropical Pacific, *Science, 282*, 59-60, 1998

Cortijo, E., L Labeyrie, L. Vidal, M. Vautravers, M Chapman, J C Duplessy, M. Elliot, M. Arnold, J -L Turon, and G Auffret, Changes in sea surface hydrology associated with Heinrich event 4 in the North Atlantic Ocean between 40° and 60°N, *Earth Planet. Sci. Lett., 146*, 29-45, 1997.

Craig, H., and L I Gordon, Deuterium and oxygen 18 variations in the ocean and the marine atmosphere, in *Stable Isotopes in Oceanographic Studies and Paleotemperatures*, edited by E. Tongiorgi, pp. 9-130, Cons. Naz. delle Rico,, Pisa, Italy, 1965

Cuffey, K M, G D Clow, R B Alley, M. Stuiver, E D Waddington, and R W Saltus, Large Arctic temperature change at the Wisconsin-Holocene glacial transition, *Science, 270*, 455-458, 1995.

Dansgaard, W, H B. Clausen, N. Gundestrup, C.U. Hammer, S.F. Johnsen, P.M. Kristinsdottir, and N Reeh, A new Greenland deep ice core, *Science, 218*, 1273-1277, 1982.

Dansgaard, W, et al., Evidence for general instability of past climate from a 250-kyr ice-core record, *Nature, 364*, 218-220, 1993.

Dietrich, G, K Kalle, W. Krauss, and G Siedler, *General Oceanography*, 626 pp., John Wiley, New York, 1975.

Dokken, T., and E Jansen, Rapid changes in the mechanism of ocean convection during the last glacial period, *Nature, 40*, 458-461, 1999.

Dowdeswell, J A, A Elverhøi, J T Andrews, and D. Hebbeln, Asynchronous deposition of ice-rafted layers in the Nordic Seas and North Atlantic Ocean, *Nature, 400*, 348-351, 1999.

Dreger, D, Decadal-to-centennial-scale sediment records of ice advance on the Barents shelf and meltwater discharge into the northeastern Norwegian Sea over the last 40 kyr, *Ber. Rep. für. Geowiss., 3*, pp 1-80, Christian-Albrechts Univ., Kiel, Germany, 1999.

Duplessy, J.C., L. Labeyrie, A Juillet-Leclerc, F. Maitre, J. Duprat, and M. Sarnthein, Surface salinity reconstruction of the North Atlantic Ocean during the Last Glacial Maximum, *Oceanol. Acta, 14*(4), 311-324, 1991.

Elliot, M, L. Labeyrie, G. Bond, E. Cortijo, J.-L. Turon, N. Tisnerat, and J.-C. Duplessy, Millennial-scale iceberg discharges in the Irminger Basin during the last glacial period: Relationship with the Heinrich events and environmental settings, *Paleoceanography, 13*(5), 433-446, 1998

Endler, R, and K.S Lackschewitz, R V. "Sonne"-cruise SO82, 1992: Geophysical investigations along the Reykjanes Ridge, North Atlantic, *Meereseswiss. Ber. 5*, 1-61, Inst. für Ostseeforschung, Warnemunde, Germany 1993

Fairbanks, R.G', A 17,000-year glacio-eustatic sea level record Influence of glacial melting rates on the Younger Dryas event and deep-ocean circulation, *Nature, 342*, 637-642, 1989.

Fillon, R.H., and J.C Duplessy, Labrador Sea bio-, tephro-, oxygen isotopic stratigraphy and late Quaternary paleoceanographic trends, *Can. J. Earth Sci., 17*, 831-854, 1980.

Fronval, T, E Jansen, J. Bloemendal, and S. Johnsen, Oceanic evidence for coherent fluctuations in Fennoscandian and Laurentide ice sheets on millennium timescales, *Nature, 374*, 443-446, 1995

Funder, S., C Hjort, J Landvik, S. Nam, N Reeh, and R. Stein, History of a stable ice margin-east Greenland during the middle and upper Pleistocene, *Quat. Sci. Rev., 17*, 77-123, 1998

Geochemical Ocean Sections Study Atlantic, Pacific and Indian Ocean expeditions, shorebased data and graphics, edited by H.G. Ostlud, et al, *Nat. Sci. Found.*, vol 7, 1987.

Greenland Ice Core Project Members, Climate instability during the last interglacial period recorded in the GRIP ice core, *Nature, 362*, 203-207, 1993.

Grootes, P.M, and M Stuiver, Oxygen 18/16 variability in Greeland snow and ice with 10^{-3} to 10^{5}-year resolution, *J. Geophys. Res., 102*(C12), 26,455-26,470, 1997

Grootes, P M, M Stuiver, J W.C. White, S. Johnsen, and J. Jouzel, Comparison of oxygen isotope records from the GISP2 and GRIP Greenland ice cores, *Nature, 366*, 552-554, 1993

Grousset, F D, L Labeyrie, J A Sinko, M Cremer, G Bond, J Duprat, E Cortijo, and S Huon, Patterns of ice-rafted detritus in the glacial North Atlantic (40°-55°N), *Paleoceanography, 8(2)*, 175-192, 1993

Gwiazda, R H, S.R Hemming, and W.S. Broecker, Provenance of icebergs during Heinrich event 3 and the contrast to their sources during other Heinrich episodes, *Paleoceanography, 11*(4), 371-378, 1996a

Gwiazda, R.H, S R Hemming, and W S Broecker, Tracking the sources of icebergs with lead isotopes The provenance of ice-rafted debris in Heinrich layer 2, *Paleoceanography, 11*(1), 77-93, 1996b

Habicht, J K A, in *Paleoclimate, Paleomagnestism, and Continental Drift*, edited by M.K. Horn, Am Assoc of Pet Geol, Tulsa, Okla., 1979

Haflidason, H, J Eiriksson, and S van Kreveld, The tephrochronology of Iceland and the North Atlantic region during the middle and late Quaternary. A review, *J Quat. Sci. 15(1)*, 3-22, 2000.

Heinrich, H, Origin and consequences of cyclic ice rafting in the northeast Atlantic ocean during the past 130,000 years, *Quat. Res., 29*, 142-152, 1988

Hemleben, C, M Spindler, and O R. Anderson, *Modern Planktonic Foraminifera*, 363 pp., Springer-Verlag, New York, 1989

Hendy, I L, and J P Kennett, Latest Quaternary North Pacific surface-water responses imply atmosphere-driven climate instability, *Geology, 27(4)*, 291-294, 1999

Heusser, L, and F Sirocko, Millennial pulsing of vegetation change in southern California. A record of Indo-Pacific ENSO events from the past 24,000 years, *Geology, 25*, 243-246, 1997.

Hopkins, T.S, The GIN Sea-A synthesis of its physical oceanography and literature review 1972-1985, *Earth Science Rev, 30*, 175-318, 1991.

Imbrie, J, J.D Hays, D.G Martinson, A. McIntyre, A C Mix, J J Morley, N G Pisias, W Prell, and N.J. Shackleton, The orbital theory of Pleistocene climate Support from a revised chronology of the marine $\delta^{18}O$ record, in *Milankovitch and Climate*, vol 1, edited by A. Berger et al, pp 269-305, D Reidel, Norwell, Mass, 1984.

Imbrie, J. et al., On the structure and origin of major glaciation cycles, 1, Linear responses to Milankovitch forcing, *Paleoceanography, 7*(6), 701-738, 1992

Johnsen, S.J, H.B Clausen, W. Dansgaard, K Fuhrer, N Gundestrup, C U. Hammer, P. Iversen, J Jouzel, B. Stauffer, and J.P. Steffensen, Irregular glacial interstadials recorded in a new Greenland ice core, *Nature, 359*, 311-313, 1992.

Jung, S.J.A., Wassermassenaustausch zwischen dem NE-Atlantik und dem Europäischen Nordmeer während der letzten 300 000/80 000 Jahre im Abbild stabiler O- und C-Isotope, *Ber Sonderforschungsber. 313*(61), 1-148, Christian-Albrechts Univ., Kiel, Germany, 1996.

Keeling, C D, An 1800-year periodicity in oceanic tidal dissipation as a possible contributor to millennial-scale global climate change, paper presented at Mechanisms of Millennial-Scale Global Climate Change, AGU Snowbird, Utah, 1998.

Kennett, J.P, and B.L. Ingram, A 20,000-year record of ocean circulation and climate change from Santa Barbara basin, *Nature, 377*, 510-514, 1995.

Krauss, W., The North Atlantic Current, *J Geophys. Res., 91*(C4), 5061-5074, 1986

Labeyrie, L.D., J C. Duplessy, and P L Blanc, Variations in mode of formation of oceanic deep waters over the past 125,000 years, *Nature, 327*, 477-482, 1987.

Lackschewitz, K S, and H -J Wallrabe-Adams, Composition and origin of volcanic ash zones in late Quaternary sediments from the Reykjanes Ridge: Evidence for ash fallout and ice-rafting, *Mar. Geol., 136*, 209-224, 1997

Lackschewitz, K.S., K.-H Baumann, B Gehrke, H.-J. Wallrabe-Adams, H. Erlenkeuser, and J Heinemeier, Late Quaternary northern ice sheet fluctuations. Evidence from short-term variations in the sediment composition of Reykjanes Ridge sediment cores, *Quat. Res., 49*, 171-182, 1998.

Lang, C., M. Leuenberger, J Schwander, and S Johnsen, 16°C rapid temperature variation in central Greenland, 70,000 years ago, *Science, 286*, 934-937,1999

Levitus, S, Climatological atlas of the world ocean, *NOAA Prof. Pap., 13*, 173 pp, U S Govt Print. Office, Washington, D C, 1982

MacAyeal, D R, Binge/purge oscillations of the Laurentide ice sheet as a cause of the North Atlantic's Heinrich events, *Paleoceanography, 8*(6), 775-784, 1993a

MacAyeal, D R, A low-order model of the Heinrich event cycle, *Paleoceanography, 8*(6), 767-773, 1993b

Mayewski, P A, et al, Changes in atmospheric circulation and ocean ice cover over the North Atlantic during the last 41,000 years, *Science, 263*, 1747-1751, 1994

Mayewski, P.A., L.D Meeker, M S Twickler, S. Whitlow, Q. Yang, W.B Lyons, and M Prentice, Major features and forcing of high-latitude Northern Hemisphere atmospheric circulation using a 110,000 year-long glaciochemical series, *J. Geophys Res., 102*(C12), 26,345-12,366, 1997

McManus, J., R Anderson, W Broecker, M Fleisher, and S. Higgins, Radiometrically determined sedimentary fluxes in the sub-polar North Atlantic during the last 140,000 years, *Earth Planet. Sci. Lett., 155*, 29-43, 1998

McManus, J., D.W Oppo, and J L. Cullen, A 0 5-million-year record of millennial-scale climate variability in the North Atlantic, *Science, 283*, 971-975, 1999

Meese, D., R Alley, T Gow, P M Grootes, P Mayewski, M. Ram, K Taylor, E Waddington, and G. Zielinski, Preliminary depth-age scale of the GISP2 ice core, *CRREL Spec. Rep. 94-1*, 66 pp, Cold Regions Res and Eng. Lab., Hanover, N.H., 1994.

Moros, M., R. Endler, K S Lackschewitz, H -J Wallrabe-Adams, J Mienert, and W Lemke, Physical properties of Reykjanes Ridge sediments and their linkage to high-resolution Greenland Ice Sheet Project 2 ice core data, *Paleoceanography, 12*(5), 687-695, 1997

Nadeau, M -J., M. Schleicher, P. Grootes, H. Erlenkeuser, A. Gottdang, D J.W. Mous, M. Sarnthein, and H. Willkomm, The Leibniz-Labor AMS facility at the Christian-Albrechts University, Kiel, Germany, *Nuclear Inst. and Meth. in Phsscis Res.*, B, 22-30, 1997

Nam, S., R. Stein, H. Grobe, and H. Hubberton, Late Quaternary glacial-interglacial changes in sediment composition at the east Greenland continental margin and their paleoceanographic implications, *Mar. Geol., 122*, 243-262, 1995.

Ninnemann, U.S., C.D. Charles, and D.A. Hodell, Origin of global millennial-scale climate events. Constraints from the Southern Ocean deep-sea sedimentary record, in *Mechanisms of Global Climate Change at Millennial Time Scales, Geophys. Monogr. Ser.*, vol. 112, edited by P.U Clark, R.S. Webb., and L D. Keigwin, pp 99-112, AGU, Washington, D.C., 1999.

Oppo, D.W., J.F. McManus, and J.L Cullen, Abrupt climate events 500,000 to 340,000 years ago. Evidence from subpolar North Atlantic sediments, *Science, 297*, 1335-1338, 1998.

Paillard, D , and L. Labeyrie, Role of the thermohaline circulation in the abrupt warming after Heinrich events, *Nature, 372*, 162-164, 1994

Pflaumann, U., J. Duprat, C. Pujol, and L D Labeyrie, SIMMAX· A modern analog technique to deduce Atlantic sea surface temperatures from planktonic foraminifera in deep-sea sediments, *Paleoceanography, 11*(1), 15-35, 1996.

Rahmstorf, S., Bifurcations of the Atlantic thermohaline circulation in response to changes in the hydrological cycle, *Nature, 378*, 145-149, 1995.

Rasmussen, T.L., E. Thomsen, L. Labeyrie, and T.C.E. van Weering, Circulation changes in the Faeroe-Shetland Channel correlating with cold events during the last glacial period (58-10 ka), *Geology, 24*, 937-940, 1996.

Rasmussen, T L., T.C.E van Weering, and L Labeyrie, Climatic instability, ice sheets and ocean dynamics at high northern latitudes during the last glacial period (58-10 ka BP), *Quat. Sci. Rev., 16*, 71-80, 1997.

Ruddiman, W.F., and L.K Glover, Vertical mixing of ice-rafted volcanic ash in North Atlantic sediments, *Geol. Soc. Am. Bull., 83*, 2817-2836, 1972.

Ruddiman, W.F , and A. McIntyre, Ice-age thermal response and climatic role of the surface Atlantic Ocean, 40°N to 63°N, *Geol. Soc. Am. Bull., 95*, 381-396, 1984.

Sarnthein, M , K. Winn, S J A. Jung, J-C Duplessy, L Labeyrie, H. Erlenkeuser, and G. Ganssen, Changes in east Atlantic deepwater circulation over the last 30,000 years. Eight time slice reconstructions, *Paleoceanography, 9*(2), 209-267, 1994.

Sarnthein, M , et al , Variations in Atlantic surface ocean paleoceanography, 50-80°N: A time-slice record of the last 30,000 years, *Paleoceanography, 10*(6), 1063-1094, 1995

Sarnthein, M , et al , Fundamental modes and abrupt changes in North Atlantic circulation and climate over the last 60 kyr–Concepts, reconstruction, and numerical modelling, in *The northern North Atlantic: A changing environment*, edited by P. Schäfer et al , Springer-Verlag, New York, in press, 2000.

Schäfer-Neth, C., and K. Stattegger, Icebergs in the North Atlantic: Modelling of sedimentary systems, in *Computerized modeling of sedimentary systems*, edited by J. Harff, W. Lemke, and K Stattegger, pp 63-78, Springer-Verlag, New York, 1998.

Schulz, H., U. von Rad, and H. Erlenkeuser, Correlation between Arabian Sea and Greenland climate oscillations of the past 110,000 years, *Nature, 393*, 54-57, 1998

Schulz, M., and K. Stattegger, Spectrum· Spectral analysis of unevenly spaced paleoclimatic time series, *Comput. Geosci., 23*(9), 929-945, 1997

Sirocko, F., D. Garbe-Schonberg, A. McIntyre, and B Molfino, Teleconnections between the subtropical monsoons and high latitude climates during the last deglaciation, *Science, 272*, 526-529, 1996.

Stein, R., S -I. Nam, H Grobe, and H. Hubberten, Late Quaternary glacial history and short-term ice-rafted debris fluctuations along the east Greenland continental margin, in *Late Quaternary Palaeoceanography of the North Atlantic Margins*, edited by J.T Andrews et al., *Geol. Soc. Spec. Publ., 111*, 135-151, 1996.

Stoner, J S , J E.T. Channell, and C. Hillaire-Marcel, The magnetic signature of rapidly deposited detrital layers from the deep Labrador Sea: Relationship to North Atlantic Heinrich Layers, *Paleoceanography, 11*(3), 309-325, 1996.

Stuiver, M., and T F Braziunas, Sun, ocean, climate and atmospheric $^{14}CO_2$ An evaluation of causal and spectral relationships, *Holocene, 3*(4), 289-305, 1993

Stuiver, M , and P Grootes, GISP2 oxygen isotope ratios, *Quat. Res., 54*(3), in press, 2000.

Trangeled, S., Oceanography of the Norwegian and Greenland Seas and Adjacent Areas, vol. II, Survey of 1870-1970 Literature, *Memo. SM-47*, Saclant ASW Res Cent , Italy, 1974.

Trauth, M H., M Sarnthein, and M. Arnold, Bioturbational mixing depth and carbon flux at the sea-floor, *Paleoceanography, 12*(3), 517-526, 1997

Veum, T , D. Jansen, A M , I Beyer, and J.C. Duplessy, Water mass exchange between the North Atlantic and the Norwegian Sea during the past 28,000 years, *Nature, 356*, 783-785, 1992.

Vidal, L., L Labeyrie, and T.C.E van Weering, Benthic $\delta^{18}O$ records in the North Atlantic over the last glacial period (60-10 kyr): Evidence for brine formation, *Paleoceanography, 13*(3), 245-251, 1998

Voelker, A H.L , Zur Deutung der Dansgaard-Oeschger Ereignisse in ultra-hochauflösenden Sedimentprofilen aus dem Europäischen Nordmeer, *Ber. Rep. Inst. für Geowiss., 9*, pp. 1-278, 1999.

Voelker, A.H.L , M Sarnthein, P. Grootes, H Erlenkeuser, C. Laj, A Mazaud, M.-J Nadeau, and M. Schleicher, Correlation of marine ^{14}C ages from the Nordic Seas with the GISP2 isotope record: Implications for ^{14}C calibration beyond 25 ka BP, *Radiocarbon, 40*(1), 517-534, 1998

Vogelsang, E., Palāo-Ozeanographie des Europäischen Nordmeeres an Hand stabiler Kohlenstoff- und Sauerstoffisotope, *Ber. Sonderforschungsber. 313*(23), pp. 1-136, Christian-Albrechts Univ , Kiel, Germany, 1990

Wang, L , M Sarnthein, H Erlenkeuser, J Grimalt, P Grootes, S Heilig, E. Ivanova, M Kienast, C Pelejero, and U Pflaumann, East Asian monsoon climate during the late Pleistocene. High-resolution sediment records from the South China Sea, *Mar. Geol., 156*, 245-284, 1999

Weinelt, M , M Sarnthein, U Pflaumann, H. Schulz, S Jung, and H. Erlenkeuser, Ice-free Nordic seas during the Last Glacial Maximum? Potential sites of deepwater formation, *Palaeoclimates, 1*, 283-309, 1996.

Welch, P D , The use of fast Fourier transform for the estimation of power spectra· A method based on time averaging over short, modified periodograms, *IEEE Transactions on Audio and Electroacoustics, 15 (2)*, 70-73, 1967.

Zielinski, G A., P A Mayewski, L D Meeker, S. Whitlow, and M S Twickler, A 110,000-yr record of explosive volcanism from the GISP2 (Greenland) ice core, *Quat Res., 45*, 109-118, 1996

Zielinski, G.A , P A Mayewski, L.D Meeker, D Grönvold, M S. Germani, S Whitlow, M S Twickler, and T K Taylor, Volcanic aerosol records and tephrochronology of the Summit, Greenland, ice cores, *J. Geophys Res., 102*(C12), 26,625-26,640, 1997

S van Kreveld, M Sarnthein, and U Pflaumann, Institut für Geowissenschaften, Christian-Albrechts Universität, Olshausenstrasse 40, D-24118 Kiel, Germany. (sk@gpi uni-kiel de, ms@gpi.uni-kiel de, up@gpi.uni-kiel.de)

H Erlenkeuser, P Grootes, M J Nadeau, and A Voelker, Leibniz-Labor fur Altersbestimmung und Isotopenforschung, Christian-Albrechts Universität, Max Eythstrasse 11-13, D-24118 Kiel, Germany (HErlenkeuser@leibniz.uni-kiel de, pgrootes@leibniz.uni-kiel.de, mnadeau@leibniz uni-kiel de, antje@sfb313.uni-kiel de)

S. Jung, Research School for Sedimentary Geology, Center for Marine Earth Sciences, Free University, De Boelelaan 1085, 1081 HV Amsterdam, The Netherlands. (jung@geo vu.nl)

(Received October 5, 1999;
revised February 17, 2000;
accepted March 22, 2000.)